

Statistical Guarantees for Reasoning Probes on Looped Boolean Circuits

Anastasis Kratsios^{1,2}, Giulia Livieri³, A. Martina Neuman^{*4}

¹Department of Mathematics, McMaster University, Canada
²Vector Institute, Canada

³The London School of Economics and Political Science

⁴University of Vienna, Faculty of Mathematics
 kratsioa@mcmaster.ca g.livieri@lse.ac.uk neumana53@univie.ac.at

Abstract

We study the statistical behaviour of reasoning probes in a stylized model of looped reasoning, given by Boolean circuits whose computational graph is a perfect ν -ary tree ($\nu \geq 2$) and whose output is appended to the input and fed back iteratively for subsequent computation rounds. A reasoning probe has access to a sampled subset of internal computation nodes—possibly without covering the entire graph—and seeks to infer which ν -ary Boolean gate is executed at each queried node, representing uncertainty via a probability distribution over a fixed collection of m admissible ν -ary gates. This partial observability induces a generalization problem, which we analyze in a realizable, transductive setting.

We show that, when the reasoning probe is parameterized by a graph convolutional network (GCN)-based hypothesis class and queries N nodes, the worst-case generalization error attains the optimal rate $\mathcal{O}(\sqrt{\log(2/\delta)}/\sqrt{N})$ with probability at least $1 - \delta$, for $\delta \in (0, 1)$. Our analysis combines snowflake metric embedding techniques with tools from statistical optimal transport. A key insight is that this optimal rate is *achievable independently of graph size*, owing to the existence of a low-distortion one-dimensional snowflake embedding of the induced graph metric. As a consequence, our results provide a sharp characterization of how structural properties of the computational graph govern the statistical efficiency of reasoning under partial access.

Keywords: Reasoning probes, looped reasoning, digraphs (directed graphs), snowflake metric embedding, hitting probability metric, statistical optimal transport, fractional Wasserstein distance, concentration of measure, optimal generalization rates, graph convolutional networks

1 Introduction

Recent advances in machine learning have placed increasing emphasis on reasoning capabilities. Prominent examples include agentic systems [61, 68], tool-augmented models [4, 40], iterative self-improvement strategies [21, 46, 65, 69, 71], and architectures incorporating relational or graph-based inductive biases [14, 33]. Concurrently, large pretrained language models—such as the GPT family [1, 20] and Gemini [29]—have demonstrated strong performance on widely used *proxies* for reasoning. As such reasoning-oriented components are embedded within increasingly complex machine learning pipelines, the need to understand and explain how these systems produce their outputs has been repeatedly emphasized by leaders in the field [13, 16].

A common toolkit for analyzing the internal computations of models used in reasoning tasks is often formulated in terms of (neural) *reasoning probes*, developed within the interpretability literature, ranging from “low-complexity” [3, 10, 25] to more sophisticated ones [26, 27, 28, 54, 55]. These probes aim to predict properties of internal representations, such as intermediate computations, at each queried node within a model. While probing methods are now well-developed as practical tools, their statistical behavior is comparatively less well understood.

We study the statistical behavior of reasoning probes in a stylized setting. Throughout, we assume intrinsic *probe uncertainty*; see Section 1.1 below. We consider the probing of looped *Boolean circuits* with a streamlined computational graph: a perfect ν -ary tree ($\nu \geq 2$), in which each computation node implements a Boolean gate with fan-in ν and fan-out 1. The circuit output is appended to the previous input and fed back for subsequent rounds of computation; see Section 1.2. We study reasoning probes parameterized by GCNs, as they encode the computational graph of the Boolean circuit into its predictions; see also Section 1.1 below.

*Corresponding author. Email: neumana53@univie.ac.at

1.1 Reasoning probe and probe uncertainty

Let $m \geq 2$. Probe outputs are modeled as elements of the relative interior Δ_m° of the m -simplex Δ_m —for a detailed definition, see Section 2—which we later interpret as encoding uncertainty over candidate gates. Each element in Δ_m represents a probability distribution over the m candidate gates, drawn from a fixed finite set. Degenerate distributions correspond to boundary points of the simplex, which lie in $\Delta_m \setminus \Delta_m^\circ$. We equip Δ_m° with the vector space structure induced by the Aitchison geometry; see Section 2 and also [31, 56, 57]. Under this geometry, the boundary of Δ_m lies at infinite distance and is therefore unattainable. This precludes degenerate distributions and enforces intrinsic uncertainty in probe outputs. All probes we consider are necessarily Lipschitz (see Proposition B.1) with respect to the hitting probability metric (see Section 2) on the directed graph associated with our looped reasoning model. In this regime, probes induce approximately homophilic gate assignments on the graph, in the sense that local neighbourhoods cannot exhibit large variations in gate distributions. This motivates our focus on GCN-based probes, which are well suited to such homophilic regimes [43].

1.2 How looped reasoning is formalized

We build on a common perspective in the theoretical foundations of AI that models “reasoning” as the emulation of circuits or algorithms computing a given task, typically realized as a computable function. Through this lens on machine reasoning, the community has established that many modern neural architectures can simulate broad classes of computations, leading to strong expressivity results. Representative examples include, the Turing machine viewpoint [17, 24, 47, 58, 62] for recursive or looped networks; Boolean [22, 45, 50, 51, 63] and general circuit-complexity lenses [42] for non-recursive architectures; and connections to mathematical logic [15, 37, 49].

By a Boolean reasoning model, we mean a circuit computing a B -bit Boolean function $f : \{0, 1\}^B \rightarrow \{0, 1\}$, represented as a *directed acyclic graph* (DAG) of Boolean gates. For example, when the circuit is a perfect ν -ary tree of height h , then $B = \nu^h$, and each internal computation node has fan-in ν and fan-out 1 Boolean gate. As a point of reference, [41, Lemma 15] shows that when $\nu = 2$, every Boolean function admits a DAG-based circuit representation, using binary gates AND, OR, and $\text{Proj}(x_1, x_2) \mapsto x_1$, with input literals allowed. In analogy with standard chain-of-thought implementations (e.g. [38, 60, 70]), and as illustrated in Figure 1, we allow for *looped* reasoning, wherein the model’s output is recursively fed back into its input for a prespecified number of iterations, generating a sequence of intermediate computational states. These intermediate outputs, initiated by a prompt of at most B bits, may be viewed as being written to a figurative reasoning *tape*. To make this intuition precise, we now give a formal description of the underlying computational architecture and its associated memory dynamics.

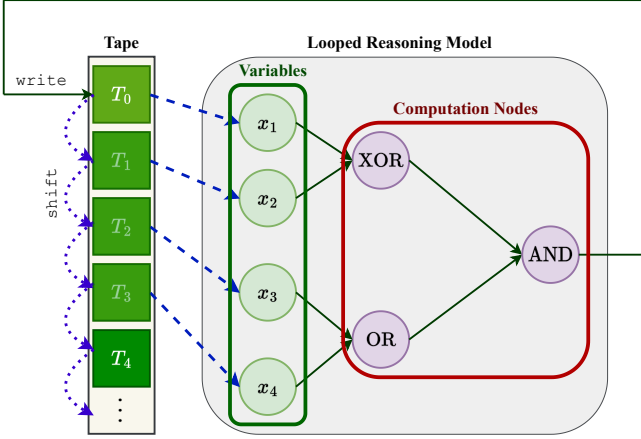
Let $B_\nu = (V_\nu, E_\nu)$ be a *perfect (full and complete)* rooted ν -ary tree of height h , with edges oriented toward the root node r (we restrict to perfect trees to simplify the treatment of nodes and related computations). The tree B_ν serves as the computation core and supports only feedforward computation. Let $T \stackrel{\text{def}}{=} \{T_0, T_1, \dots\}$ be a potentially infinite tape representing *latent computation memory*. For discrete time $t \in \mathbb{N}_{\geq 0}$, let $B_\nu^{(t)}$ (resp. $r^{(t)}$) and $T^{(t)}$ denote time-indexed *copies* of the computation tree (resp. root) and the memory tape, respectively. The looping mechanism governing the evolution of the system is specified, for $t \in \mathbb{N}_{\geq 0}$, $i \in \mathbb{N}_{\geq 0}$, by the following operations *in order*:

$$\begin{aligned} \text{read} &: T^{(t)} \rightarrow B_\nu^{(t)} \\ \text{shift} &: T^{(t)} \rightarrow T^{(t+1)} \quad \text{where} \quad T_i^{(t)} \mapsto T_{i+1}^{(t+1)} \\ \text{write} &: B_\nu^{(t)} \rightarrow T^{(t+1)} \quad \text{where} \quad r^{(t)} \mapsto T_0^{(t+1)}. \end{aligned} \tag{1}$$

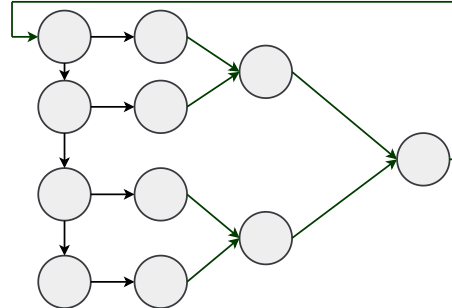
First, the **read** operation maps the current memory tape into the computation tree. Second, the **shift** operation updates the memory tape, where each tape cell is shifted forward. Finally, the **write** operation maps the root output of the computation tree back to memory, where the root value is written to the first tape cell. Informally, (1) defines a *causal evolution* $(B_\nu^{(t)}, T^{(t)}) \mapsto (B_\nu^{(t+1)}, T^{(t+1)})$. See Figure 1(a). Moreover, the **read** operation is encoded by an underlying DAG structure $G^{(t)} = (V^{(t)}, E^{(t)})$:

$$V^{(t)} = \{T_i^{(t)} : i \in [\nu^h]_0\} \cup V_\nu^{(t)} \quad \text{and} \quad E^{(t)} = \{(T_i^{(t)}, v_{i+1}^{(t)}) : i \in [\nu^h]_0\} \cup E_\nu^{(t)}. \tag{2}$$

Here, $[\nu^h]_0 \stackrel{\text{def}}{=} \{0, 1, \dots, \nu^h - 1\}$, and $v_i^{(t)}$ denotes the time- t copy of the base (input) tree node v_i , taking Boolean values. Thus, from (2) at any given time t , only the first ν^h tape positions are connected to the computation core. Assume that each internal computation node $v \in V_\nu \setminus \{v_1, v_2, \dots, v_{\nu^h}\}$ is assigned a Boolean gate $g_v : \{0, 1\}^\nu \rightarrow \{0, 1\}$, independent of time step and drawn from a fixed finite prescribed set. Then at each time step, the feedforward evaluation of these gates on the current inputs realizes a ν^h -Boolean function. Finally, let $\mathcal{G}^{\text{time}}$ denote the directed graph obtained by combining the intra-time edges $E^{(t)}$ with the inter-time edges induced by the **shift** and **write**



(a) *Looped reasoning model*



(b) *Strongly connected digraph $\mathcal{G}^{\text{time}}/\mathbb{N}_{\geq 0}$*

Figure 1: A looped reasoning model (a) and its induced time-quotient, strongly connected digraph (b). In the looped reasoning model in (a), at time step $t \in \mathbb{N}$, the bits stored at the tape positions $T_0^{(t)}, T_1^{(t)}, \dots, T_3^{(t)}$ are fed as input variables at the base nodes of a perfect binary rooted tree (green nodes). The computation nodes (red-framed box) apply binary gates; the output at root $\mathbf{r}^{(t)}$ (purple node with AND operation) is fed back to tape $T_0^{(t+1)}$.

operations; this graph captures the global information flow induced by looping. Then the time-quotient graph $\mathcal{G}^{\text{time}}/\mathbb{N}_{\geq 0}$ is a *strongly connected* digraph $G_{\text{sc}} = (V_{\text{sc}}, E_{\text{sc}})$, where

$$\begin{aligned} V_{\text{sc}} &\stackrel{\text{def}}{=} V_{\nu} \cup \{T_i\}_{i \in [\nu^h]_0} \\ E_{\text{sc}} &\stackrel{\text{def}}{=} E_{\nu} \cup \{(\mathbf{r}, T_0)\} \cup \{(T_i, T_{i+1})\}_{i \in [\nu^h]_0} \cup \{(T_i, v_{i+1})\}_{i \in [\nu^h]_0}. \end{aligned} \quad (3)$$

See Figure 1(b). In this way, the looped execution embeds the feedforward Boolean circuit into a strongly connected directed graph.

1.3 Contributions

Main contribution We establish statistical generalization guarantees for GCN-parameterized reasoning probes (Theorem 3.1). In particular, our results show that, despite the potentially exponential size of the computational graph, GCN-parameterized reasoning probes can achieve statistically optimal $\mathcal{O}(1/N^{1/2})$ rates independent of graph cardinality.

Secondary contributions Our analysis relies on two technical developments of independent interest. First, we obtain a one-dimensional snowflake embedding for finite metric spaces. Second, we derive Lipschitz estimates for GCNs on digraphs; to the best of our knowledge, these are the first such results.

Taken together, these results position metric geometry as the governing factor in the statistical efficiency of learning under partial access.

1.4 Organization of paper

Section 2 introduces all notation and background needed to formalize our main results. Section 3 presents our main result (Theorem 3.1). Technical discussions on our proof technique are provided in Section 4. All proofs and additional theoretical background are deferred to the appendix.

2 Preliminaries

We review the essential preliminary concepts and conventions. We write \mathbb{N} to denote the set of natural numbers, $\mathbb{N}_{\geq 0}$ to denote the set of non-negative integers, and $\mathbb{R}_{\geq 0}$ to denote the set of non-negative reals. Let $k \in \mathbb{N}$. We have used $[k]_0$ to denote the index set of cardinality k starting from 0. We also write $[k] \stackrel{\text{def}}{=} \{1, 2, \dots, k\}$ to denote the index set of cardinality k starting from 1. For a finite set V , we denote by $\#V$ its cardinality.

We use boldface letters to denote Euclidean vectors, e.g. $\mathbf{p}, \mathbf{x}, \mathbf{Y}$, and write $\|\mathbf{x}\|_\infty$ for the ℓ^∞ -norm of \mathbf{x} . For a linear operator $W : \mathbb{R}^m \rightarrow \mathbb{R}^n$, identified as a matrix $W \in \mathbb{R}^{n \times m}$, we define $\|W\|_{\text{op}} \stackrel{\text{def}}{=} \sup_{x \in \mathbb{R}^m \setminus \{\mathbf{0}\}} \|W\mathbf{x}\|_\infty / \|\mathbf{x}\|_\infty$ to be the induced ℓ^∞ -operator norm, satisfying

$$\|W\|_{\text{op}} = \max_{i=1,\dots,n} \sum_{j=1}^m |W_{i,j}|. \quad (4)$$

In our discussion of matrices generated by vertex relationships in graphs, we allow flexibility in how matrix entries are referred to. For example, when the vertices are indexed, we write $[A]_{i,j}$ or alternatively $[A]_{v_i, v_j}$. When explicit indexing is unnecessary or cumbersome, we simply write $[A]_{v,w}$ to denote an entry in A associated with the vertex pair (v, w) .

Finally, for $A, B > 0$, we write $A \lesssim B$ to indicate that there exists an absolute constant $C > 0$ such that $A \leq CB$, and $A \asymp B$ to mean both $A \lesssim B$ and $B \lesssim A$.

Strongly connected digraphs A directed graph or a digraph $G = (V, E)$ consists of a vertex set V and an edge set $E \subset V \times V$, where each edge is an ordered pair indicating direction. We always assume G to be *simple*, i.e., it contains no self-loops and no multiple directed edges (i, j) . A digraph is strongly connected if for every $i, j \in V$, there exists a directed path from i to j , and a directed path from j to i . An example of a (simple) strongly connected digraph is $G_{\text{sc}} = (V_{\text{sc}}, E_{\text{sc}})$ given in (3).

Strongly connected digraph as metric space Let $G = (V, E)$ be a strongly connected digraph, with irreducible stochastic transition matrix P_G (8) and Perron vector ϕ . Suppose $\#V = k$. Let $(X_n)_{n \in \mathbb{N}_0}$ be a discrete-time Markov chain on V with $\mathbb{P}(X_{n+1} = j | X_n = i) = [P_G]_{i,j}$. The *hitting time* for $i \in V$ is a random variable $\tau_i \stackrel{\text{def}}{=} \inf\{n \in \mathbb{N} : X_n = i\}$. Let $Q_G \in \mathbb{R}^{k \times k}$ be,

$$[Q_G]_{i,j} \stackrel{\text{def}}{=} \mathbb{P}[\tau_j < \tau_i | X_0 = i] \quad \text{for } i, j \in [k]. \quad (5)$$

Let $E_G \in \mathbb{R}^{k \times k}$ be the normalized hitting probabilities matrix, such that

$$[E_G]_{i,j} \stackrel{\text{def}}{=} \phi(i)[Q_G]_{i,j} = \phi(j)[Q_G]_{ji} \quad \text{if } i \neq j \quad (6)$$

[18, Lemma 1.1] and $[E_G]_{i,i} \stackrel{\text{def}}{=} 1$. Then by [18, Theorem 1.3], the *hitting probability metric*

$$d_G(i, j) \stackrel{\text{def}}{=} -\log([E_G]_{i,j}) \quad (7)$$

is a metric on G . In general, the metric encodes the *global graph connectivity* induced by the long-term behavior of the associated directed Markov chain.

Graph Laplacians Let $G = (V, E)$ be a strongly connected digraph, with $\#V = k$. The *adjacency matrix* $A_G \in \mathbb{R}^{k \times k}$ is defined by $[A_G]_{i,j} = 1$ if $(i, j) \in E$ and $[A_G]_{i,j} = 0$ otherwise. The associated *degree matrix* is diagonal, with $[D_G]_{i,i} \stackrel{\text{def}}{=} \sum_{j=1}^k [A_G]_{i,j}$. Then for a strongly connected digraph G , the *row-stochastic transition matrix*

$$P_G \stackrel{\text{def}}{=} D_G^{-1} A_G \quad (8)$$

is *irreducible*, i.e., for every $i, j \in V$, there exists $l \in \mathbb{N}$ such that $[P_G^l]_{i,j} > 0$. Thus, P has a unique positive left eigenvector ϕ with the eigenvalue 1, normalized by [23, Section 2],

$$\sum_{i \in V} \phi(i) = 1, \quad (9)$$

known as the *Perron vector* or the invariant distribution of P_G . Let $\Phi_G \in \mathbb{R}^{k \times k}$ be diagonal such that $\Phi_G(i, i) \stackrel{\text{def}}{=} \phi(i)$. Following [23], define the *combinatorial Laplacian* by

$$\Delta_G \stackrel{\text{def}}{=} \Phi_G - \frac{\Phi_G P_G + P_G^\top \Phi_G^\top}{2} = \Phi_G - \frac{\Phi_G P_G + P_G^\top \Phi_G}{2} \quad (10)$$

where M^\top denotes the transpose of M . Evidently, Δ_G is a real-valued symmetric matrix.

Remark 2.1. One may alternatively consider the normalized graph Laplacian [23], $\Delta_G^n \stackrel{\text{def}}{=} \Phi_G^{-1/2} \Delta_G \Phi_G^{-1/2}$. We do not pursue this choice here, since the ℓ^∞ -operator norm (4) of Δ_G^n can grow rapidly, for $G = G_{\text{sc}}$ (3); see (62), (63) in Appendix B.

Graph convolutional networks on digraphs Let $k \in \mathbb{N}$, and let \mathcal{G}_k be the set of simple, strongly connected digraphs on $[k]$. For each $G = (V, E) \in \mathcal{G}_k$, where we identify $V = [k]$, let Δ_G be the combinatorial Laplacian in (10). For $p \in \mathbb{N}$, let Δ_G^p be the p -power of Δ_G . We consider the following common GCN model; see [44, Chapter 5.3].

Definition 2.1. Let $L, p, d_{\text{in}}, d_{\text{out}} \in \mathbb{N}$. Let $\beta_1, \dots, \beta_L > 0$. For $l = 0, 1, \dots, L$, let $d_l \in \mathbb{N}$, with $d_0 \stackrel{\text{def}}{=} d_{\text{in}}$, $d_L \stackrel{\text{def}}{=} d_{\text{out}}$. Let $E_{\text{in}} \subset \mathbb{R}^{d_{\text{in}}}$ and $E_{\text{out}} \subset \mathbb{R}^{d_{\text{out}}}$. For $l = 1, 2, \dots, L$, let $W_l \in \mathbb{R}^{d_l \times d_{l-1}}$ be given weight matrices, with $\|W_l\|_{\text{op}} \leq \beta_l$. Let $\sigma : \mathbb{R} \rightarrow \mathbb{R}$ be a given 1-Lipschitz activation function. We consider the maps $f_{\text{GCN}} : \mathcal{G}_k \times E_{\text{in}}^k \rightarrow E_{\text{out}}^k \subset \mathbb{R}^{d_{\text{out}} \times k}$ defined by generalized GCNs with p -hop graph convolution, activation σ , network parameters (W_1, \dots, W_L) , and network size is given by $(\beta_1, \dots, \beta_L)$. These maps admit the following iterative representation. For $G \in \mathcal{G}_k$ and $\mathbf{x} \in E_{\text{in}}^k$, let $f_{\text{GCN}}(G, \mathbf{x}) \stackrel{\text{def}}{=} \mathbf{H}_L \stackrel{\text{def}}{=} W_L \mathbf{H}_{L-1}$, where

$$\mathbf{H}_{l+1} \stackrel{\text{def}}{=} \mathcal{L}_{l+1}(\mathbf{H}_l) \quad \text{for } l = 0, 1, \dots, L-2, \quad \text{and} \quad \mathbf{H}_0 \stackrel{\text{def}}{=} \mathbf{x}. \quad (11)$$

Here, $\mathcal{L}_l(\tilde{\mathbf{x}}) \stackrel{\text{def}}{=} \sigma \bullet (W_l(\Delta_G^p \tilde{\mathbf{x}}^\top)^\top)$, for $\tilde{\mathbf{x}} \in \mathbb{R}^{d_l \times k}$, where \bullet denotes component-wise application.

Aitchison geometry For $\mathfrak{m} \in \mathbb{N}$ with $\mathfrak{m} \geq 2$, let $\Delta_{\mathfrak{m}} \stackrel{\text{def}}{=} \{\mathbf{p} \in \mathbb{R}^{\mathfrak{m}} : p_i \geq 0, \sum_{i=1}^{\mathfrak{m}} p_i = 1\}$ be the \mathfrak{m} -simplex. The relative interior of $\Delta_{\mathfrak{m}}$ is

$$\Delta_{\mathfrak{m}}^\circ \stackrel{\text{def}}{=} \{\mathbf{p} \in \mathbb{R}^{\mathfrak{m}} : p_i > 0 \text{ and } \sum_{i=1}^{\mathfrak{m}} p_i = 1\}. \quad (12)$$

It is well-known that $\Delta_{\mathfrak{m}}^\circ$ is an $(\mathfrak{m} - 1)$ -dimensional simplex embedded in a linear subspace admitting the *Helmert basis* [2], [48, Section 14.1]

$$\mathbf{e}^i \stackrel{\text{def}}{=} \sqrt{\frac{i}{i+1}} \left(\underbrace{\frac{1}{i}, \dots, \frac{1}{i}}_{i \text{ entries}}, -1, 0, \dots, 0 \right) \quad \text{for } i = 1, 2, \dots, \mathfrak{m} - 1.$$

Inspired by [34], we further turn $\Delta_{\mathfrak{m}}^\circ$ into a *Hilbert space* with the *Aitchison inner product*

$$\langle \mathbf{p}, \mathbf{q} \rangle_A \stackrel{\text{def}}{=} \frac{1}{2\mathfrak{m}} \sum_{i=1}^{\mathfrak{m}} \sum_{j=1}^{\mathfrak{m}} \log\left(\frac{p_i}{p_j}\right) \log\left(\frac{q_i}{q_j}\right).$$

Then $\Delta_{\mathfrak{m}}^\circ$, equipped with the *Aitchison norm* $\|\cdot\|_A \stackrel{\text{def}}{=} \sqrt{\langle \cdot, \cdot \rangle_A}$, is a metric space with the induced *Aitchison metric*

$$d_A(\mathbf{p}, \mathbf{q}) = \|\mathbf{p} - \mathbf{q}\|_A. \quad (13)$$

When equipped with the Aitchison geometry [2], $\Delta_{\mathfrak{m}}^\circ$ is isometrically isomorphic to $\mathbb{R}^{\mathfrak{m}-1}$ with its Euclidean metric [57]. We briefly record this identification. Let $\mathbb{H}^{\mathfrak{m}-1} \stackrel{\text{def}}{=} \{\mathbf{x} \in \mathbb{R}^{\mathfrak{m}} : \sum_{i=1}^{\mathfrak{m}} x_i = 0\}$. Let $\text{clr} : \Delta_{\mathfrak{m}}^\circ \rightarrow \mathbb{H}^{\mathfrak{m}-1}$ denote the *centered log-ratio* transform that is

$$\text{clr}(\mathbf{p}) \stackrel{\text{def}}{=} \left(\log p_i - \frac{1}{\mathfrak{m}} \sum_{j=1}^{\mathfrak{m}} \log p_j \right)_{i=1}^{\mathfrak{m}}. \quad (14)$$

Projecting clr onto the Helmert basis defines the *isometric log-ratio* transform $\text{ilr} : (\Delta_{\mathfrak{m}}^\circ, d_A) \rightarrow (\mathbb{R}^{\mathfrak{m}-1}, d_2)$,

$$\text{ilr}(\mathbf{p}) \stackrel{\text{def}}{=} (\langle \text{clr}(\mathbf{p}), \mathbf{e}^i \rangle_2)_{i=1}^{\mathfrak{m}-1}, \quad (15)$$

where $\langle \cdot, \cdot \rangle_2$ denotes the standard Euclidean inner product and d_2 the usual Euclidean distance. We henceforth freely identify $\Delta_{\mathfrak{m}}^\circ$ with the Euclidean space $\mathbb{R}^{\mathfrak{m}-1}$ for convenience.

3 Setup and main result

Recall the computation loop $G_{\text{sc}} = (V_{\text{sc}}, E_{\text{sc}})$ introduced in (3) and the associated perfect rooted ν -ary tree $\mathbf{B}_\nu = (V_\nu, E_\nu)$ of height \mathbf{h} . The total number of vertices in V_{sc} is

$$\#V_{\text{sc}} = k = \frac{2\nu^{\mathbf{h}+1} - \nu^{\mathbf{h}} - 1}{\nu - 1}. \quad (16)$$

We fix an identification of V_{sc} with the index set $[k]$, chosen so that the first $1 + \nu + \nu^2 + \dots + \nu^h$, or $k - \nu^h$, indices correspond to the nodes V_ν of \mathcal{B}_ν , ordered hierarchically from the base level upward. One convenient choice is

$$\underbrace{1, 2, \dots, \nu^h}_{\text{base nodes}}, \underbrace{\nu^h + 1, \nu^h + 2, \dots, \nu^h + \nu^{h-1}}_{\text{level 1 nodes}}, \dots, \underbrace{k - \nu^h}_{\text{root } \mathbf{r}}, \quad (17)$$

where the base node v_i is connected to the tape position T_{i-1} , for $i = 1, 2, \dots, \nu^h$. We allow mixed notation, in which we continue to refer to the root as \mathbf{r} and the tape-nodes as T_i . Let $\Gamma \stackrel{\text{def}}{=} V_\nu \setminus \{v_1, v_2, \dots, v_{\nu^h}\}$, consisting precisely of the computation nodes in \mathcal{B}_ν . Let $\mathfrak{G} = \{\mathfrak{g}^1, \dots, \mathfrak{g}^m\}$ be a finite gate set. A *gate configuration* is a mapping $\mathcal{C} : v \mapsto \mathfrak{g}_v$ from Γ into \mathfrak{G} . We assume this configuration is given but unknown. Let $\eta \in (0, 1)$ be a certainty level. To avoid triviality, we exclude the case of perfect certainty $\eta = 1$ and no certainty $\eta = 0$. The *reasoning probe operation* $Q_\eta : V \rightarrow \Delta_m^\circ$ returns a noisy categorical description at a node $v \in V$ defined by

$$Q_\eta(v) \stackrel{\text{def}}{=} \left(\eta \cdot \mathbf{1}_{\{\mathfrak{g}_v = \mathfrak{g}^i\}} + \frac{1-\eta}{m-1} \cdot \mathbf{1}_{\{\mathfrak{g}_v \neq \mathfrak{g}^i\}} \right)_{i=1}^m.$$

Thus Q_η provides local but uncertain information about \mathcal{C} . We assume a *bounded-complexity condition* on Q_η , namely

$$\|Q_\eta(v) - Q_\eta(w)\|_A \leq K_h, \quad \text{for } v, w \in \Gamma, \quad (18)$$

where K_h grows at most exponentially in terms of h . Let $\mu_{[k]}$ be a probability measure on $[k]$ with support equal to Γ . Let¹ $\mu \stackrel{\text{def}}{=} (\mathbb{1} \times Q_\eta) \# \mu_{[k]}$, and suppose we are given independent random samples²

$$(V_1, \mathbf{P}_1), \dots, (V_N, \mathbf{P}_N) \sim \mu, \quad (19)$$

taking values on $\Gamma \times \Delta_m^\circ$; that is, $\mathbf{P}_i = Q_\eta(V_i)$. We write μ^N to denote the empirical version of μ . Let $J : \Delta_m^\circ \times \Delta_m^\circ \rightarrow \mathbb{R}_{\geq 0}$ be a loss function satisfying

$$|J(\mathbf{y}, \mathbf{z}) - J(\mathbf{y}', \mathbf{z}')| \leq C_J \max\{\|\mathbf{y} - \mathbf{y}'\|_A, \|\mathbf{z} - \mathbf{z}'\|_A\}, \quad (20)$$

for some $C_J > 0$. For $\alpha \in (0, 1)$, let $J_\alpha : \Delta_m^\circ \times \Delta_m^\circ \rightarrow \mathbb{R}_{\geq 0}$ by $J_\alpha(\mathbf{y}, \mathbf{z}) \stackrel{\text{def}}{=} J(\mathbf{y}, \mathbf{z})^\alpha$ be a *snowflaked* loss. Note that the resulting loss increases sensitivity to discrepancies at fine scales. When $\alpha = 1/2$, the resulting square-root loss has been used in [12, 66]. Given a configuration \mathcal{C} , we assume that at time $t \in \mathbb{N}$, a temporal input is applied at the base nodes of \mathcal{B}_ν . This input propagates through \mathcal{B}_ν , generating a Boolean output at each $v \in \Gamma$. We collect these outputs into a vector $\mathbf{x} \in \{0, 1\}^{s_{\nu, h}}$ where $s_{\nu, h} \stackrel{\text{def}}{=} \frac{\nu^h - 1}{\nu - 1}$. *Treating each such time step as a stand-alone experimental trial induced by the underlying configuration \mathcal{C}* , we study the (static) *transductive generalization gap* over a set of graph learners trained on \mathbf{x} at time $t \in \mathbb{N}$ and values of Q_η at sampled computation nodes.

Let $G_\Gamma \subset G_{\text{sc}}$ be the induced subgraph on Γ . Recall the general GCN model f_{GCN} in Definition 2.1, with depth $L \in \mathbb{N}$ and network parameters $(\beta_1, \dots, \beta_L)$. Set $d_{\text{in}} = 1$, $d_{\text{out}} = m - 1$. We define a hypothesis set \mathcal{H} for Q_η consisting of

$$h \stackrel{\text{def}}{=} (\mathbf{1}_{s_{\nu, h}} \otimes \text{ilr}^{-1}) \circ f_{\text{GCN}}(G_\Gamma, \cdot), \quad (21)$$

where $\mathbf{1}_{s_{\nu, h}}$ denotes the $s_{\nu, h}$ -dimensional vector of ones, and ilr is given in (15). By definition (21), $E_{\text{in}} = \{0, 1\}$ and $E_{\text{out}} \subset \Delta_m^\circ$. For $h \in \mathcal{H}$, we take the empirical risk to be

$$\mathcal{R}_{\mathbf{x}, t}^{\alpha, N}(h) \stackrel{\text{def}}{=} \frac{1}{N} \sum_{i=1}^N J_\alpha(\pi_{V_i} \circ h, \mathbf{P}_i), \quad (22)$$

and the corresponding population risk to be

$$\mathcal{R}_{\mathbf{x}, t}^\alpha(h) \stackrel{\text{def}}{=} \mathbb{E}_{(V, \mathbf{P}) \sim \mu} [J_\alpha(\pi_V \circ h, \mathbf{P})]. \quad (23)$$

The *worst-case* discrepancy between these two risks is captured by the transductive generalization gap over \mathcal{H}

$$\sup_{h \in \mathcal{H}} |\mathcal{R}_{\mathbf{x}, t}^\alpha(h) - \mathcal{R}_{\mathbf{x}, t}^{\alpha, N}(h)|. \quad (24)$$

Our main result provides an explicit upper bound on the generalization gap in terms of the problem parameters, as follows.

¹This means that μ is the push-forward of $\mu_{[k]}$ under $(\mathbb{1} \times Q_\eta)$.

²We assume sampling with replacement and that the sampling distribution μ is well-behaved, in the sense that no single point carries disproportionately arbitrarily large mass. See Section 4.

Theorem 3.1 (Main result). *Let $\alpha \in (0, 1)$. Let $t, N \in \mathbb{N}$. For every $\delta \in (0, 1)$, the following event holds with probability at least $1 - \delta$*

$$\sup_{h \in \mathcal{H}} |\mathcal{R}_{\mathbf{x}, t}^\alpha(h) - \mathcal{R}_{\mathbf{x}, t}^{\alpha, N}(h)| \lesssim \left(C_J \left(\max \left\{ \mathfrak{m}^{1/2} \left(\frac{3 + \nu}{2} \right)^{p(L-1)} \prod_{l=1}^L \beta_l, \nu^h, K_h \right\} \right)^{5/2} \right)^\alpha \left(\frac{1}{\sqrt{N}} + \frac{\sqrt{\log(2/\delta)}}{\sqrt{N}} \right). \quad (25)$$

The proof of Theorem 3.1 is given in Appendix B.

We now provide a discussion of the main result, including its interpretation and proof strategy.

4 Interpretation and proof strategy of main theorem

Uniform graph-size-independent generalization rates The analysis underlying Theorem 3.1 is *time-uniform* and applies to all $\mathbf{x} \in \{0, 1\}^{s_{\nu, h}}$ obtained, without leveraging accumulated information across rounds³. Moreover, the parameter $\alpha \in (0, 1)$ in (25) is tunable and may be selected a priori. In particular, choosing $\alpha \asymp h^{-1}$ keeps the majorant constant uniformly controlled as h grows and guarantees meaningful convergence. *To our knowledge, this is the first instance in which such dimension- or cardinality-free rates are established for reasoning probes operating on looped, strongly connected computation graphs.*

Contextual discussion on coverage property of i.i.d. sampling With computational efficiency in mind, we consider i.i.d. (memoryless) probing of vertices. Unlike systematic exploration or uniform sampling without replacement—which enforces non-revisitation and guarantees full coverage after k queries at the cost of storing previously visited vertices—i.i.d. sampling incurs no storage overhead. Under this scheme, the total number of probes N may exceed ν^h , the order of the total number of computational nodes, and even satisfy $N \gg \nu^h$ without guaranteeing full coverage. In particular, repeated sampling of a small subset of vertices may dominate, leading to highly unbalanced visitation frequencies. This phenomenon is classical in occupancy problems; see, for example, [19, Proposition 1]. While arbitrarily ill-conditioned distributions are theoretically admissible, in practice users rarely deploy strategies assigning vanishing mass to a large fraction of vertices. (*We emphasize that our generalization bounds do not require uniform coverage or coupon-collector-type guarantees, and remain valid even when many vertices are never observed.*)

Since the sampling distribution is chosen by the user, it is natural to ask how many probes are required to visit every vertex with high probability, and how this requirement depends on the sampling strategy. In this context, the classical *coupon collector problem* [32, 59] shows that for any $\bar{\delta} \in (0, 1)$,

$$N = \Theta \left(k \log \left(\frac{k}{1 - \bar{\delta}} \right) \right) \quad (26)$$

uniform samples are necessary and sufficient to cover all k vertices with probability at least $\bar{\delta}$. However, as noted above, the decisive factor is not the number of vertices alone, but the smallest probability with which any vertex is sampled.

We state the following proposition as a *non-asymptotic* formulation of [59]. It avoids the intricate combinatorial expressions appearing in [32] and [19], which involve Stirling numbers of the second kind, and presents (26) in a transparent form that makes the dependence on the minimal sampling probability, which is $\min_{i \in [k]} w_i$ below, explicit. *The proposition is recorded for completeness and its results are not used in the proof of our main theorem.*

Proposition 4.1. *Let $\mu = \sum_{i=1}^k w_i \delta_{x_i}$ be a probability measure on a k -point set \mathcal{X} , with $k \geq 2$ and $\min_{i \in [k]} w_i > 0$. Let $(X_j)_{j=1}^\infty$ be a sequence of i.i.d. random variables on \mathcal{X} with law μ . Let $\bar{\tau} \stackrel{\text{def}}{=} \inf\{n \in \mathbb{N} : \{X_j\}_{j=1}^n = \mathcal{X}\}$ be the first covering time. Then for all $\bar{n} \in \mathbb{N}$ such that $\bar{n} \geq k$,*

$$1 - k \left(1 - \min_{i \in [k]} w_i \right)^{\bar{n}} \leq \mathbb{P}(\bar{\tau} \leq \bar{n}) \leq 1 - \left(1 - \min_{i \in [k]} w_i \right)^{\bar{n}}. \quad (27)$$

The lower bound above is maximized under the uniform distribution, i.e. $w_i = 1/k$ for all $i \in [k]$. Moreover, if there exist $\bar{n} \in \mathbb{N}$ and $\bar{\delta} \in (0, 1)$ such that $\min_{i \in [k]} w_i \leq 1 - (1 - \delta)^{1/\bar{n}}$, we have $\mathbb{P}(\bar{\tau} \leq \bar{n}) \leq \bar{\delta}$.

³On the other hand, learning under feedback—where inputs depend on past outputs—would require additional assumptions on the permissible configurations.

In fact, a sharper lower bound than that in (27) can be derived and may be of independent interest:

$$1 - (k-1)^{\bar{n}} \left(\min_{i \in [k]} w_i \right)^{\bar{n}} - (k-1) \left(1 - \min_{i \in [k]} w_i \right)^{\bar{n}} \leq \mathbb{P}(\bar{\tau} \leq \bar{n}). \quad (28)$$

The proofs of Proposition 4.1 and (28) can be found in Appendix C.

A metric embedding-based proof strategy Our proof adopts a geometric strategy inspired by recent developments in metric embedding methods in learning theory. We briefly review related ideas from the literature, and then outline the proof strategy. Viewing both μ and μ^N as measures on a finite metric space, the central idea is to relate the worst-case generalization gap—uniformly over the hypothesis class—between the true risk and the empirical risk to a Wasserstein distance between μ and μ^N . This perspective frames generalization as a statistical optimal transport problem, where the main technical challenge is to control the concentration of the Wasserstein distance. Existing results are predominantly qualitative, including a central limit theorem [64]. Few non-asymptotic guarantees are available; see e.g. [39]. There, the Wasserstein distance between μ and μ^N is mapped to a corresponding Wasserstein distance in Euclidean space, for which classical optimal transport theory provides sharp concentration results. Specifically, for $m \geq 3$, the Wasserstein distance tightly concentrates around its expectation, which scales as $\mathcal{O}(1/N^{1/m})$; for $m = 2$, the rate is $\mathcal{O}(\log_2(N)/N^{1/2})$; and for $m = 1$, the optimal rate $\mathcal{O}(1/N^{1/2})$ holds. The resulting generalization bounds in [39], akin to standard Occam-type bounds, depend on the cardinality of the underlying metric space. This hierarchy of rates highlights the intrinsic cost of high dimensionality and motivates reducing the effective dimension.

More recently, [30] removes the dependence on metric cardinality by adopting a fractional 1/2-Wasserstein distance. In their approach, both the true and empirical risks are measured with respect to the 1/2-snowflaked loss function, and—by combining the results of [36] with Kantorovich duality—the resulting generalization gap is controlled by a multiple of the corresponding 1/2-Wasserstein distance in Euclidean space. At present, the analysis therein incurs a logarithmic factor in N , arising from a reduction to two dimensions; comparable rates are well-known in classical Rademacher- and Gaussian-complexity bounds [6, 7, 8, 9]. Here, we follow the same general strategy, but observe that the relevant metric space admits an α -snowflake representation in one dimension, for $\alpha \in (0, 1)$. Specifically, we show that the graph metric space G_Γ , viewed as a subgraph of G_{sc} and equipped with the *snowflaked* hitting-probability metric (see (7)) $d_{G_{sc}}^\alpha$, embeds into (\mathbb{R}, d_∞) , where d_∞ is the absolute value metric. This permits access to the optimal one-dimensional Wasserstein convergence rate of $\mathcal{O}(1/N^{1/2})$.

Broadly, our proof for Theorem 3.1 proceeds in two steps:

Step 1: We construct a one-dimensional bi-Lipschitz embedding of $(G_\Gamma, d_{G_{sc}}^\alpha)$ with minimal distortion (given in Proposition A.1 for general finite metric space). This step combines Assouad-type embedding techniques for doubling metric spaces [53] with low-dimensional embedding results for snowflaked metrics [35]. An illustration is given in Figure 2.

Step 2: Following the reduction in Step 1, we control the worst-case generalization gap (24) by the corresponding one-dimensional α -Wasserstein distance. As an intermediate step, we estimate the Lipschitz regularity of the model f_{GCN} and diameter of the digraph G_Γ ; both quantities contribute, in part, to the majorant constant in (25).

5 Conclusion

This paper establishes *statistical guarantees for reasoning probes* in a concrete and structured model of looped reasoning, namely Boolean circuits whose computational graph is a perfect ν -ary rooted tree, for $\nu \geq 2$. We consider reasoning probes whose hypotheses are parameterizable by GCNs, allowing the probe to encode the underlying circuit geometry. Within this setting, we analyze the problem of inferring which Boolean gates are executed at

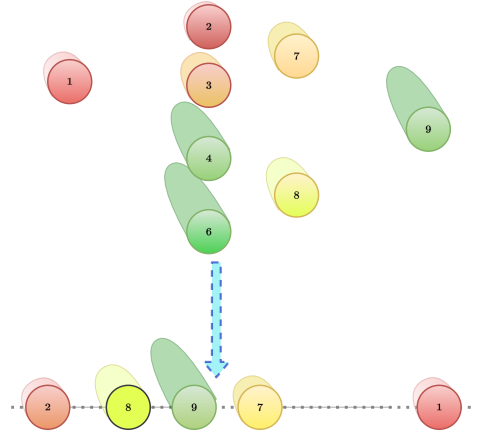


Figure 2: Illustration of a one-dimensional embedding of a finite metric space; the objective is to keep metric distortion small.

Figure 2: Illustration of a one-dimensional embedding of a finite metric space; the objective is to keep metric distortion small.

internal computation nodes when only a subset of those nodes is observable. Our main result (Theorem 3.1) shows that the internal gate structure of a looped circuit can be statistically inferred in a generalization sense from partial observations, even under intrinsic uncertainty in the probe outputs. In particular, when N nodes are queried, the worst-case generalization error decays at the optimal central-limit-theorem rate $\mathcal{O}(1/\sqrt{N})$ independently of the total size of the circuit, with a priori tuning of the snowflake parameter.

Our analysis refines the geometric learning framework of [30] (see also [39] for related work). On the technical front, a key contribution is the construction of a low-distortion one-dimensional snowflake embedding of the circuit’s induced graph metric (Proposition A.1), which yields an optimal surrogate learning problem on the real line. This embedding can be viewed as an ultra-low-dimensional counterpart to the embeddings in [53] and, more broadly, as an ℓ^∞ version of Assouad-type embeddings [5, 52]. This result allows us to reduce the original graph-based generalization problem to a concentration-of-measure analysis for fractional Wasserstein distances on a finite metric space (Proposition A.2), providing a non-asymptotic route complementary to the theory of [64], which does not rely on embedding techniques. By combining sharp concentration bounds with explicit control of the probe’s Lipschitz constant, derived from the digraph geometry of the circuit (Proposition B.1), we obtain optimal sample complexity rates with favourable constants. In the contextual discussion of Section 4, we study which sampling distribution minimizes the number of i.i.d. node queries required to visit all nodes with high probability. We show that the uniform distribution is optimal in this sense (Proposition 4.1), situating this result within the coupon-collection literature [19, 32, 59].

5.1 Future work

Our results provide a rigorous stepping stone toward general transductive learning guarantees for reasoning probes. Natural directions for future work include extending the analysis to broader classes of looped reasoning models, as well as to alternative probe architectures beyond GCNs.

A particularly compelling longer-term direction is the development of principled tools for identifying *undesirable* internal reasoning behaviors—such as redundant, degenerate, or unsafe patterns—from a small number of queries of a model’s internal computation graph. From a statistical perspective, our generalization guarantees provide a useful reference for such analyses: because they are model-agnostic within a broad probe class and achieve optimal rates under minimal assumptions, they serve as baseline guarantees upon which more specialized detection or auditing procedures may be built. Establishing statistical guarantees for such detection problems remains largely open, and we view the present work as a foundational step toward this goal.

6 Acknowledgements

The authors would like to thank Gautam Kamath for his super-helpful feedback on the early stages of the paper. A. M. Neuman acknowledges the financial support from the Austrian Science Fund (FWF) under Project P 37010. A. Kratsios acknowledges the financial support from an NSERC Discovery Grants No. RGPIN-2023-04482, No. DGECR-2023-00230, and from the project Bando PRIN 2022 named “Qnt4Green - Quantitative Approaches for Green Bond Market: Risk Assessment, Agency Problems and Policy Incentives”, codice 2022JRY7EF, CUP E53D23006330006, funded by European Union – NextGenerationEU, M4c2.

A Supplementary preliminaries on Wasserstein concentration

Let $(\mathcal{X}, d_{\mathcal{X}})$ be a metric space, and let $\text{diam}(\mathcal{X}) \stackrel{\text{def}}{=} \sup_{x,y} d_{\mathcal{X}}(x, y)$ be its diameter. For $\alpha \in (0, 1]$, we regard $(\mathcal{X}, d_{\mathcal{X}}^\alpha)$ as the α -snowflaked version of $(\mathcal{X}, d_{\mathcal{X}})$, where $d_{\mathcal{X}}^\alpha(x, y) \stackrel{\text{def}}{=} d_{\mathcal{X}}(x, y)^\alpha$. The α -Hölder Wasserstein distance between two probability measures λ, λ' on \mathcal{X} is given by (see [36, Definition 9])⁴

$$\mathcal{W}_\alpha(\lambda, \lambda') \stackrel{\text{def}}{=} \sup_{f \in H(\alpha, \mathcal{X}, 1)} \mathbb{E}_{X \sim \lambda}[f(X)] - \mathbb{E}_{Y \sim \lambda'}[f(Y)], \quad (29)$$

where, for $C \geq 0$, $H(\alpha, \mathcal{X}, C)$ denotes the set of real-valued α -Hölder continuous functions f on \mathcal{X} satisfying

$$|f(x) - f(y)| \leq C d_{\mathcal{X}}(x, y)^\alpha, \quad (30)$$

for every $x, y \in \mathcal{X}$. If $\alpha = 1$ then $H(1, \mathcal{X}, C) = \text{Lip}(\mathcal{X}, C)$, the set of real-valued C -Lipschitz continuous functions on \mathcal{X} . Note that definition (30), and thus (29), depends on the metric choice. For example, if \mathcal{X} have been equipped with $d_{\mathcal{X}}^\alpha$, then (30) would describe a C -Lipschitz function on $(\mathcal{X}, d_{\mathcal{X}}^\alpha)$.

The following lemma is the main result of this appendix section and provides the key ingredient in the proof of Theorem 3.1.

Lemma A.1. *Let $\alpha \in (0, 1)$. Let $(\mathcal{X}, d_{\mathcal{X}})$ be a k -point metric space, with $k \geq 2$. Suppose $1 \leq d_{\mathcal{X}}(x, y)$ for every $x \neq y \in \mathcal{X}$. Let λ be a probability measure on \mathcal{X} , and let λ^N be its associated empirical measure. Then the following holds for every $\delta \in (0, 1)$ and $N \in \mathbb{N}$,*

$$\mathcal{W}_\alpha(\lambda, \lambda^N) \lesssim \text{diam}(\mathcal{X})^{3\alpha/2} \cdot \left(\frac{1}{\sqrt{N}} + \frac{\sqrt{\log(2/\delta)}}{\sqrt{N}} \right) \quad (31)$$

with probability at least $1 - \delta$.

The proof of Lemma A.1 relies on two main steps. First, we map $(\mathcal{X}, d_{\mathcal{X}}^\alpha)$ bi-Lipschitz-ly to (\mathbb{R}, d_∞) , where d_∞ denotes the ℓ^∞ -metric. Second, we apply a known result for the Wasserstein distance \mathcal{W}_1 in (\mathbb{R}, d_∞) . These steps are developed in Propositions A.1 and A.2 below.

Proposition A.1 (Low distortion snowflake-embedding into \mathbb{R}). *Let $\alpha \in (0, 1)$. Let $(\mathcal{X}, d_{\mathcal{X}})$ be a k -point metric space with $k \geq 2$. Suppose $1 \leq d_{\mathcal{X}}(x, y) \leq D$ for $x \neq y \in \mathcal{X}$. Then there exists a threshold $\theta_* \in (0, 1)$ depending on α and \mathcal{X} such that the following holds. For every $\theta \in (\theta_*, 1)$, there exists a bi-Lipschitz embedding $\varphi_{\alpha, \theta} : (\mathcal{X}, d_{\mathcal{X}}^\alpha) \rightarrow (\mathbb{R}, d_\infty)$ satisfying*

$$\begin{aligned} (1 + 1/20)^{-3/2} (1 + \theta)^{-1} D^{-\alpha/2} d_{\mathcal{X}}(x, y)^\alpha &\leq |\varphi_{\alpha, \theta}(x) - \varphi_{\alpha, \theta}(y)| \\ &\leq (1 + 1/20)^{3/2} (1 + \theta) d_{\mathcal{X}}(x, y)^\alpha. \end{aligned} \quad (32)$$

Particularly, $\text{diam}(\varphi_{\alpha, \theta}(\mathcal{X})) \leq (1 + 1/20)^{3/2} (1 + \theta) D^\alpha$.

Proposition A.2. *Let \mathcal{X} be a compact subset of \mathbb{R} . Let λ be a probability measure on \mathcal{X} , and let λ^N be its empirical measure. Then for all $t > 0$ and all $N \geq 4$,*

$$\mathbb{P}\left(\left|\mathcal{W}_1(\lambda, \lambda^N) - \mathbb{E}[\mathcal{W}_1(\lambda, \lambda^N)]\right| \geq t\right) \leq 2e^{-\frac{2Nt^2}{\text{diam}(\mathcal{X})^2}},$$

and

$$\mathbb{E}[\mathcal{W}_1(\lambda, \lambda^N)] \leq \frac{\sqrt{2}\text{diam}(\mathcal{X})}{\sqrt{N}}. \quad (33)$$

Proposition A.2 is a key technical variant of [36, Lemma 16], adapted to the setting of (\mathbb{R}, d_∞) , and is established in [30, Lemma B.2]. Proposition A.1 presents a bi-Lipschitz embedding result of potential independent interest for $(\mathcal{X}, d_{\mathcal{X}}^\alpha)$ into (\mathbb{R}, d_∞) , whose proof is given below. The proof of Lemma A.1 then follows immediately.

⁴Definition (29) is inspired by the fact that setting $\alpha = 1$ recovers the dual definition [67, Remark 6.5] of the Wasserstein \mathcal{W}_1 transport distance [67, Definition 6.1].

Proof of Proposition A.1. Assume first $\alpha \neq 1/2$. We construct a bi-Lipschitz embedding $\varphi_{\alpha,\theta} : (\mathcal{X}, d_{\mathcal{X}}^\alpha) \rightarrow (\mathbb{R}, d_\infty)$ via the composition of the following bi-Lipschitz maps:

$$(\mathcal{X}, d_{\mathcal{X}}^\alpha) \rightarrow (\mathbb{R}^{m_\alpha}, d_\infty) \rightarrow (\mathbb{R}^{m_\alpha}, d_\infty^{1/2}) \rightarrow (\mathbb{R}, d_\infty), \quad (34)$$

where m_α is to be determined. Some of the results invoked below are stated in terms of the *doubling constant*⁵. Since we work exclusively with k -point metric spaces with $k \geq 2$, we only require the fact that their doubling constants are at least 2 and at most k (see e.g. [30, Example 2.2]). For the first embedding map in (34), we appeal to the ℓ^∞ version of Assouad's Embedding Theorem due to [53, Theorem 3]. This result ensures that for every $\alpha \in (0, 1)$, there exists a bi-Lipschitz embedding $\psi_\alpha : (\mathcal{X}, d_{\mathcal{X}}^\alpha) \rightarrow (\mathbb{R}^{m_\alpha}, d_\infty)$ with distortion at most $1 + 1/20$ and

$$m_\alpha = \left\lceil \frac{M^{6+\log_2 20}}{\alpha(1-\alpha)} \right\rceil, \quad (35)$$

where $M \geq 2$ denotes the doubling constant of $(\mathcal{X}, d_{\mathcal{X}})$. The exponent of M in (35) can be deduced from the proof of [53, Theorem 3] together with [53, Proposition 2]. In particular, under either the upper- or lower-normalized distortion convention⁶, we obtain

$$(1 + 1/20)^{-1} d_{\mathcal{X}}(x, y)^\alpha \leq \|\psi_\alpha(x) - \psi_\alpha(y)\|_\infty \leq (1 + 1/20) d_{\mathcal{X}}(x, y)^\alpha, \quad (36)$$

and therefore,

$$\text{diam}(\psi_\alpha(\mathcal{X})) \leq (1 + 1/20) \text{diam}(\mathcal{X})^\alpha. \quad (37)$$

Turning to the second embedding in (34), we consider the identity map $\iota : (\psi_\alpha(\mathcal{X}), d_\infty) \rightarrow (\psi_\alpha(\mathcal{X}), d_\infty^{1/2})$. Since $(\psi_\alpha(\mathcal{X}), d_\infty)$ is a k -point metric space, this map is automatically bi-Lipschitz. Indeed, we can estimate its bi-Lipschitz constants as follows. From (36) and that $1 \leq d_{\mathcal{X}}(x, y) \leq D$ for $x \neq y \in \mathcal{X}$,

$$(1 + 1/20)^{-1} D^{-\alpha} \leq \|\psi_\alpha(x) - \psi_\alpha(y)\|_\infty^{-1} \leq (1 + 1/20).$$

Thus,

$$\begin{aligned} (1 + 1/20)^{-1/2} D^{-\alpha/2} \|\psi_\alpha(x) - \psi_\alpha(y)\|_\infty &\leq \|\iota \circ \psi_\alpha(x) - \iota \circ \psi_\alpha(y)\|_\infty^{1/2} \\ &= \|\psi_\alpha(x) - \psi_\alpha(y)\|_\infty \|\psi_\alpha(x) - \psi_\alpha(y)\|_\infty^{-1/2} \\ &\leq (1 + 1/20)^{1/2} \|\psi_\alpha(x) - \psi_\alpha(y)\|_\infty. \end{aligned} \quad (38)$$

Moreover, (37), (38) imply

$$\text{diam}(\iota \circ \psi_\alpha(\mathcal{X})) \leq (1 + 1/20)^{3/2} D^\alpha. \quad (39)$$

Let M' be the doubling constant of $(\psi_\alpha(\mathcal{X}), d_\infty)$. Although it can be verified from (36), (38) that M' is at most a constant power of M , we only need that $M' \geq 2$, which holds since $(\psi_\alpha(\mathcal{X}), d_\infty)$ is a k -point metric space with $k \geq 2$. Continuing to the last embedding in (34), we invoke [35, Theorem 6.6] and its proof, which implies that for every $\theta \in (0, 1)$ ⁷, there exists a bi-Lipschitz embedding $\psi_\theta : (\iota \circ \psi_\alpha(\mathcal{X}), d_\infty^{1/2}) \rightarrow (\mathbb{R}^{m_\theta}, d_\infty)$ with distortion at most $1 + \theta$, where

$$1 \leq m_\theta \leq \lfloor \theta^{-C^* \log_2(M')} \rfloor, \quad (40)$$

and $C^* > 1$ is an absolute constant⁸. Let $\theta'_* \stackrel{\text{def}}{=} 1/2^{1/C^* \log_2(M')}$. We see that if $\theta \in (\theta'_*, 1)$,

$$\theta^{C^* \log_2(M')} > \left(\frac{1}{2^{1/C^* \log_2(M')}} \right)^{C^* \log_2(M')} = \frac{1}{2}, \quad (41)$$

since $M' \geq 2$. Thus, for θ in this range, (40) implies that $m_\theta = \lfloor \theta^{-C^* \log_2(M')} \rfloor = 1$ and yields a bi-Lipschitz embedding $\psi_\theta : (\iota \circ \psi_\alpha(\mathcal{X}), d_\infty^{1/2}) \rightarrow (\mathbb{R}, d_\infty)$ that is

$$\begin{aligned} (1 + \theta)^{-1} \|\iota \circ \psi_\alpha(x) - \iota \circ \psi_\alpha(y)\|_\infty^{1/2} &\leq |\psi_\theta \circ \iota \circ \psi_\alpha(x) - \psi_\theta \circ \iota \circ \psi_\alpha(y)| \\ &\leq (1 + \theta) \|\iota \circ \psi_\alpha(x) - \iota \circ \psi_\alpha(y)\|_\infty^{1/2}. \end{aligned} \quad (42)$$

⁵ $(\mathcal{X}, d_{\mathcal{X}})$ is doubling with the doubling constant $M \in \mathbb{N}$, if for every $r \geq 0$ and every $x \in \mathcal{X}$, the closed ball $B(x, r) \stackrel{\text{def}}{=} \{y \in \mathcal{X} : d_{\mathcal{X}}(x, y) \leq r\}$ can be covered by some M closed balls $B(x_1, r/2), \dots, B(x_M, r/2)$, i.e. $B(x, r) \subset \bigcup_{i=1}^M B(x_i, r/2)$, and if M is the smallest such number.

⁶In the upper-normalized convention, $(1 + \theta)^{-1} d(x, y) \leq d(f(x), f(y)) \leq d(x, y)$, while in the lower-normalized convention, $d(x, y) \leq d(f(x), f(y)) \leq (1 + \theta)d(x, y)$, where $1 + \theta$ is a given distortion.

⁷The fourth paragraph of the proof of [35, Theorem 6.6] implicitly assumes that the distortion $1 + \theta$ lies in $(1, 2)$.

⁸This follows from the proof of [35, Theorem 6.6].

Let $\varphi_{\alpha,\theta} \stackrel{\text{def}}{=} \psi_\theta \circ \iota \circ \psi_\alpha$. Then combining (36), (38), (42), we obtain (32), while combining (39), (42) yields the final claim on the diameter.

Assume now $\alpha = 1/2$. We directly embed $(\mathcal{X}, d_{\mathcal{X}}^{1/2})$ into (\mathbb{R}, d_∞) by adapting the last embedding in (34). In particular, we let $\theta_* \stackrel{\text{def}}{=} 1/2^{1/C^* \log_2(\mathbb{M})}$, where $\mathbb{M} \geq 2$ is the doubling constant of $(\mathcal{X}, d_{\mathcal{X}})$. Arguing as in (40), (41), if $\theta \in (\theta_*, 1)$, then $m_\theta = \lfloor \theta^{-C^* \log_2(\mathbb{M})} \rfloor = 1$. This yields, by [35, Theorem 6.6], a bi-Lipschitz embedding $\varphi_{1/2,\theta} \stackrel{\text{def}}{=} \psi_\theta : (\mathcal{X}, d_{\mathcal{X}}^{1/2}) \rightarrow (\mathbb{R}, d_\infty)$. \square

Proof of Lemma A.1. The proof is adapted from the argument in [30, Proposition 4.1]. We recall Proposition A.1, which states that for each $\theta \in (\theta_*, 1)$, there exist a bi-Lipschitz embedding $\varphi_{\alpha,\theta} : (\mathcal{X}, d_{\mathcal{X}}^\alpha) \rightarrow (\mathbb{R}, d_\infty)$, such that

$$\text{diam}(\varphi_{\alpha,\theta}(\mathcal{X})) \leq \mathbf{S} \text{diam}(\mathcal{X})^\alpha, \quad (43)$$

where $\mathbf{S} \stackrel{\text{def}}{=} (1 + 1/20)^{3/2}(1 + \theta)$. We also set $\mathbf{R} \stackrel{\text{def}}{=} (1 + 1/20)^{-3/2}(1 + \theta)^{-1} \text{diam}(\mathcal{X})^{-\alpha/2}$. Define $\gamma \stackrel{\text{def}}{=} (\varphi_{\alpha,\theta})_\#(\lambda)$ and $\gamma^N \stackrel{\text{def}}{=} (\varphi_{\alpha,\theta})_\# \lambda^N$, which are probability measures on the k -point metric space $(\varphi_{\alpha,\theta}(\mathcal{X}), d_\infty) \subset (\mathbb{R}, d_\infty)$. By combining (43) with Proposition A.2, we obtain

$$\mathbb{E}[\mathcal{W}_1(\gamma, \gamma^N)] \leq \frac{\sqrt{2} \text{diam}(\varphi_{\alpha,\theta}(\mathcal{X}))}{\sqrt{N}} \leq \frac{\sqrt{2} \mathbf{S} \text{diam}(\mathcal{X})^\alpha}{\sqrt{N}} \quad (44)$$

and for each $t > 0$,

$$\mathbb{P}(|\mathcal{W}_1(\gamma, \gamma^N) - \mathbb{E}[\mathcal{W}_1(\gamma, \gamma^N)]| \geq t) \leq 2e^{-\frac{2Nt^2}{\mathbf{S}^2 \text{diam}(\mathcal{X})^{2\alpha}}} \leq 2e^{-\frac{Nt^2}{16 \text{diam}(\mathcal{X})^{2\alpha}}}. \quad (45)$$

We translate (44), (45) into expressions of Wasserstein distances between λ, λ^N as follows. By Proposition A.1, $\varphi_{\alpha,\theta}$ is \mathbf{S} -Lipschitz on $(\mathcal{X}, d_{\mathcal{X}}^\alpha)$, and its inverse $\varphi_{\alpha,\theta}^{-1}$ is \mathbf{R}^{-1} -Lipschitz on $(\varphi_{\alpha,\theta}(\mathcal{X}), d_\infty)$. It follows that, if $f \in \mathcal{H}(\alpha, \mathcal{X}, 1)$ (30), then $f \circ \varphi_{\alpha,\theta}^{-1} \in \mathcal{H}(1, \varphi_{\alpha,\theta}(\mathcal{X}), \mathbf{R}^{-1})$, and conversely, if $f \circ \varphi_{\alpha,\theta}^{-1} \in \mathcal{H}(1, \varphi_{\alpha,\theta}(\mathcal{X}), 1)$, then $f \in \mathcal{H}(\alpha, \mathcal{X}, \mathbf{S})$. Indeed, for $x, y \in \varphi_{\alpha,\theta}(\mathcal{X})$,

$$|f \circ \varphi_{\alpha,\theta}^{-1}(x) - f \circ \varphi_{\alpha,\theta}^{-1}(y)| \leq d_{\mathcal{X}}(\varphi_{\alpha,\theta}^{-1}(x), \varphi_{\alpha,\theta}^{-1}(y))^\alpha \leq \mathbf{R}^{-1} |x - y|,$$

and for $x, y \in \mathcal{X}$,

$$|f(x) - f(y)| = |f \circ \varphi_{\alpha,\theta}^{-1}(\varphi_{\alpha,\theta}(x)) - f \circ \varphi_{\alpha,\theta}^{-1}(\varphi_{\alpha,\theta}(y))| \leq |\varphi_{\alpha,\theta}(x) - \varphi_{\alpha,\theta}(y)| \leq \mathbf{S} d_{\mathcal{X}}(x, y)^\alpha.$$

Therefore, by a change of variables, we get

$$\mathcal{W}_\alpha(\lambda, \lambda^N) \leq \mathbf{R}^{-1} \mathcal{W}_1(\gamma, \gamma^N) \quad \text{and} \quad \mathcal{W}_1(\gamma, \gamma^N) \leq \mathbf{S} \mathcal{W}_\alpha(\lambda, \lambda^N). \quad (46)$$

By definition, $\mathbf{S}, \mathbf{S}^{-1} \asymp 1$, and $\mathbf{S}, \mathbf{S}^{-1} \leq \mathbf{R}^{-1}$, and $\mathbf{R}^{-1} \asymp \text{diam}(\mathcal{X})^{\alpha/2}$. Thus, on the one hand, combining (44), (46) yields

$$\mathbb{E}[\mathcal{W}_\alpha(\lambda, \lambda^N)] \leq \frac{C \text{diam}(\mathcal{X})^{3\alpha/2}}{\sqrt{N}}, \quad (47)$$

for some absolute $C > 0$. On the other hand, combining (44), (45), (46) allows us to derive, for $t > 0$,

$$\begin{aligned} \mathcal{W}_\alpha(\lambda, \lambda^N) - \mathbb{E}[\mathcal{W}_\alpha(\lambda, \lambda^N)] &\leq \mathbf{R}^{-1} \mathcal{W}_1(\gamma, \gamma^N) - \mathbf{S}^{-1} \mathbb{E}[\mathcal{W}_1(\gamma, \gamma^N)] \\ &\leq (\mathbf{R}^{-1} - \mathbf{S}^{-1}) \mathbb{E}[\mathcal{W}_1(\gamma, \gamma^N)] + \mathbf{R}^{-1} t \\ &\leq \frac{C \text{diam}(\mathcal{X})^{3\alpha/2}}{\sqrt{N}} + \text{diam}(\mathcal{X})^{\alpha/2} t, \end{aligned} \quad (48)$$

for some absolute $C > 0$, which happens with probability at least $1 - 2e^{-Nt^2/(16 \text{diam}(\mathcal{X})^{2\alpha})}$. Writing $\mathcal{W}_\alpha(\lambda, \lambda^N) = \mathbb{E}[\mathcal{W}_\alpha(\lambda, \lambda^N)] + \mathcal{W}_\alpha(\lambda, \lambda^N) - \mathbb{E}[\mathcal{W}_\alpha(\lambda, \lambda^N)]$ and combining with (47), (48), we obtain the desired conclusion. \square

B Proof of main theorem

Proof of Theorem 3.1. The proof proceeds along the lines of [30, Theorem 3.1]. Define a metric on $G_{\text{sc}} \times \Delta_m^\circ$ by

$$d_{G_{\text{sc}} \times \Delta_m^\circ}((v, \mathbf{p}), (w, \mathbf{q})) \stackrel{\text{def}}{=} \max\{d_{G_{\text{sc}}}(v, w), d_A(\mathbf{p}, \mathbf{q})\},$$

where $d_{G_{sc}}$ denotes the hitting probability metric (7) on G_{sc} and d_A the Aitchison metric (13). Let $\mathcal{D} \stackrel{\text{def}}{=} \{(v, Q_\eta(v)) : v \in \Gamma\}$ inherit the induced metric. For $h \in \mathcal{H}$, we associate $J_h : \Gamma \times \Delta_{\mathfrak{m}}^\circ \rightarrow \mathbb{R}_{\geq 0}$, defined to be $J_h(v, \mathbf{p}) \stackrel{\text{def}}{=} J(\pi_v \circ h(\mathbf{x}), \mathbf{p})^{1/2}$. Then $J_h|_{\mathcal{D}}$ is a function of $v \in \Gamma$ —indeed,

$$(J_h|_{\mathcal{D}})(v, \mathbf{p}) = J_h(v, Q_\eta(v)) = J(\pi_v \circ h(\mathbf{x}), Q_\eta(v))^{1/2}.$$

By recalling (22), (23) and that $\mu = (\mathbb{1} \times Q_\eta)_\# \mu_{[k]}$ (19) and μ^N are both supported on Γ , we interpret

$$\mathcal{R}_{\mathbf{x},t}^\alpha(h) = \mathbb{E}_{(V,\mathbf{P}) \sim \mu}[J_h(V, \mathbf{P})] \quad \text{and} \quad \mathcal{R}_{\mathbf{x},t}^{\alpha,N}(h) = \mathbb{E}_{(V,\mathbf{P}) \sim \mu^N}[J_h(V, \mathbf{P})].$$

Observe the following. Suppose $J_h|_{\mathcal{D}}$ is \mathbf{C}_J^* -Lipschitz, for $\mathbf{C}_J^* > 0$, i.e.

$$|J(\pi_v \circ h(\mathbf{x}), Q_\eta(v)) - J(\pi_w \circ h(\mathbf{x}), Q_\eta(w))| \leq \mathbf{C}_J^* d_{G_{sc}}(v, w). \quad (49)$$

Then by invoking Kantorovich-Rubinstein duality [67, Remark 6.5 and Theorem 5.10(i)], we obtain

$$|\mathcal{R}_{\mathbf{x},t}^\alpha(h) - \mathcal{R}_{\mathbf{x},t}^{\alpha,N}(h)| \leq (\mathbf{C}_J^*)^\alpha \mathcal{W}_\alpha(\mu, \mu^N), \quad (50)$$

where the Wasserstein distance \mathcal{W}_α is given in (29). Applying Lemma A.1 to the metric space $(\mathcal{D}, d_{G_{sc}} \times \Delta_{\mathfrak{m}}^\circ|_{\mathcal{D}})$, we deduce that for every $\delta \in (0, 1)$,

$$\mathcal{W}_\alpha(\mu, \mu^N) \lesssim \text{diam}(\mathcal{D})^{3\alpha/2} \cdot \left(\frac{1}{\sqrt{N}} + \frac{\sqrt{\log(2/\delta)}}{\sqrt{N}} \right) \quad (51)$$

holds with probability at least $1 - \delta$. Substituting (51) into (50) and taking the supremum over $h \in \mathcal{H}$ gives

$$\sup_{h \in \mathcal{H}} |\mathcal{R}_{\mathbf{x},t}^\alpha(h) - \mathcal{R}_{\mathbf{x},t}^{\alpha,N}(h)| \lesssim (\mathbf{C}_J^* \text{diam}(\mathcal{D})^{3/2})^\alpha \cdot \left(\frac{1}{\sqrt{N}} + \frac{\sqrt{\log(2/\delta)}}{\sqrt{N}} \right), \quad (52)$$

with the same probability. Thus to complete the argument, we estimate $\text{diam}(\mathcal{D})$ and \mathbf{C}_J^* in (52). For the latter, if for every $h \in \mathcal{H}$ and every $v, w \in \Gamma$, $\|\pi_v \circ h(\mathbf{x}) - \pi_w \circ h(\mathbf{x})\|_A \leq \mathbf{C}_H d_{G_{sc}}(v, w)$, and if $\|Q_\eta(v) - Q_\eta(w)\|_A \leq \mathbf{C}_{Q_\eta} d_{G_{sc}}(v, w)$, for some $\mathbf{C}_H, \mathbf{C}_{Q_\eta} > 0$, then for $(v, Q_\eta(v)), (w, Q_\eta(w)) \in \mathcal{D}$,

$$\begin{aligned} |J(\pi_v \circ h(\mathbf{x}), Q_\eta(w)) - J(\pi_w \circ h(\mathbf{x}), Q_\eta(w))| &\leq \mathbf{C}_J \|\pi_v \circ h(\mathbf{x}) - \pi_w \circ h(\mathbf{x})\|_A \\ &\leq \mathbf{C}_J \mathbf{C}_H d_{G_{sc}}(v, w), \end{aligned} \quad (53)$$

and

$$|J(\pi_v \circ h(\mathbf{x}), Q_\eta(v)) - J(\pi_v \circ h(\mathbf{x}), Q_\eta(w))| \leq \mathbf{C}_J \|Q_\eta(v) - Q_\eta(w)\|_A \leq \mathbf{C}_J \mathbf{C}_{Q_\eta} d_{G_{sc}}(v, w). \quad (54)$$

Combining (49), (53), (54), together with the triangle inequality, we arrive at an upper bound:

$$\mathbf{C}_J^* \leq \mathbf{C}_J (\mathbf{C}_H + \mathbf{C}_{Q_\eta}). \quad (55)$$

It remains to estimate the quantities $\text{diam}(\mathcal{D})$, \mathbf{C}_H , \mathbf{C}_{Q_η} , which are provided in the following proposition.

Proposition B.1. *It holds that*

- (i) $\text{diam}(\mathcal{D}) \lesssim \max\{\nu^h, K_h\}$,
- (ii) $\mathbf{C}_{Q_\eta} \leq K_h$,
- (iii) $\mathbf{C}_H \leq 2(\mathfrak{m} - 1)^{1/2} \left(\frac{3+\nu}{2}\right)^{p(L-1)} \prod_{l=1}^L \beta_l$.

The proof of Proposition B.1 is given below. An application of (55) and Proposition B.1 to (52) then gives (25) as desired. \square

Proof of Proposition B.1. For notational convenience, we write the (v, w) -entry of a matrix A as $A(v, w)$ for all matrices under consideration below.

Proof of Proposition B.1(i). Suppose

$$\text{diam}(G_{\text{sc}}) \lesssim \nu^h, \quad (56)$$

which yields $\text{diam}(\Gamma) \leq \text{diam}(G_{\text{sc}}) \lesssim \nu^h$. Since (18) holds and since $\nu \geq 2$, it follows that

$$\text{diam}(\mathcal{D}) \leq \max\{\text{diam}(\Gamma), K_h\} \lesssim \max\{\nu^h, K_h\},$$

proving part (i). Thus in what follows, we establish (56). Although one can verify that $\text{diam}(\Gamma) \asymp \nu^h$, see Remark B.1, the computation of $\text{diam}(G_{\text{sc}})$ is more straightforward.

Recall the identification (17) of V_{sc} with the index set $[k]$, under which $v_1, v_2, \dots, v_{\nu^h}$ denote the base nodes of the computation tree B_ν , with v_i connected to the tape position T_{i-1} . We also recall our convention of mixed notation: nodes corresponding to tape positions are still referred to by T_i , and the tree root by \mathbf{r} . We begin with an estimate of the Perron vector ϕ of the irreducible stochastic transition matrix $P_{G_{\text{sc}}}$ (8). By stationary, $\phi^\top P_{G_{\text{sc}}} = \phi^\top$, that is

$$\phi(v) = \sum_{w:(w,v) \in E_{\text{sc}}} \phi(w) P_{G_{\text{sc}}}(w, v). \quad (57)$$

If all the nodes w in (57) have only one outgoing edge (w, v) in G_{sc} —meaning, $P_{G_{\text{sc}}}(w, v) = 1$ —then (57) reduces to

$$\phi(v) = \sum_{w:(w,v) \in E_{\text{sc}}} \phi(w). \quad (58)$$

By construction, the nodes v satisfying (58) are precisely

$$S \stackrel{\text{def}}{=} V_{\text{sc}} \setminus \{T_1, \dots, T_{\nu^h-1}, v_1, \dots, v_{\nu^h-1}\} = \Gamma \cup \{T_0\}.$$

In particular, inductive application of (58) across the computation tree layers, together with the positivity of ϕ , gives

$$\phi(v) \leq \phi(\mathbf{r}) \quad \text{for } v \in V_\nu. \quad (59)$$

In fact, one can argue that $\phi(v) \leq \phi(\mathbf{r})$, for every $v \in G_{\text{sc}}$, but this is not needed immediately. Moreover, for $v \in V_{\text{sc}} \setminus S$, we have $P_{G_{\text{sc}}}(w, v) = 1/2$ for all $(w, v) \in E_{\text{sc}}$ appearing in (57), and hence

$$\phi(v) = \sum_{w:(w,v) \in E_{\text{sc}}} \phi(w)/2. \quad (60)$$

Applying (58) to T_0 , and noting that there is a single outgoing edge (\mathbf{r}, T_0) , we obtain

$$\phi(T_0) = \phi(\mathbf{r}). \quad (61)$$

Using (61), we invoke (60) to $v \in V_{\text{sc}} \setminus S = \{T_1, \dots, T_{\nu^h-1}, v_1, \dots, v_{\nu^h-1}\}$, which yields

$$\phi(T_i) = \phi(v_i) = \phi(T_{i-1})/2 = \phi(\mathbf{r})/2^i \quad \text{for } i = 1, 2, \dots, \nu^h - 1. \quad (62)$$

At the same time, applying (58) to v_{ν^h} , and using that (T_{ν^h-1}, v_{ν^h}) is the unique outgoing edge, leads to

$$\phi(v_{\nu^h}) = \phi(\mathbf{r})/2^{\nu^h-1}. \quad (63)$$

From (58), (62), (63), and the fact that $\nu \geq 2$, it follows that for every node v at computation layer $l = 1$, we have

$$\frac{\phi(\mathbf{r})}{2^{\nu^h-2}} \leq \frac{2^{\nu-1}}{2^{\nu^h-1}} \cdot \phi(\mathbf{r}) = \sum_{i=0}^{\nu-2} \frac{\phi(\mathbf{r})}{2^{\nu^h-1-i}} + \frac{\phi(\mathbf{r})}{2^{\nu^h-1}} \leq \phi(v) \leq \sum_{i=1}^{\nu} \frac{\phi(\mathbf{r})}{2^i} = \left(1 - \frac{1}{2^\nu}\right) \cdot \phi(\mathbf{r}). \quad (64)$$

Proceeding inductively through the higher layers, and noting (59), we gather for v in computation layer $l = 1, 2, \dots, h-1$,

$$\frac{\nu^{l-1}}{2^{\nu^h-2}} \cdot \phi(\mathbf{r}) \leq \phi(v) \leq \min \left\{ \left(1 - \frac{1}{2^\nu}\right) \cdot \nu^{l-1}, 1 \right\} \cdot \phi(\mathbf{r}). \quad (65)$$

In view of (62), (63), (64), (65), the smallest values of $\phi(v)$ occur when $v = T_{\nu^h-1}, v_{\nu^h-1}, v_{\nu^h}$. Next, we derive estimates for several key entries of $Q_{G_{\text{sc}}}$ (5). We observe the following. Starting from \mathbf{r} , a probability mass is injected into the graph. The mass first traverses the edge (\mathbf{r}, T_0) . At each tape position T_i , for $i = 0, 1, \dots, \nu^h - 2$, the outgoing mass is split uniformly between two outgoing edges (T_i, T_{i+1}) and (T_i, v_{i+1}) . At the tape position

T_{ν^h-1} , the outgoing mass travels along the one outgoing edge (T_{ν^h-1}, v_{ν^h}) in G_{sc} . Consequently, the mass reaching T_i equals $1/2^i$, and the mass exiting to the base node v_{i+1} equals $1/2^{i+1}$, for $i = 0, 1, \dots, \nu^h - 2$, while the base node v_{ν^h} receives mass $1/2^{\nu^h-1}$. Equivalently,

$$\begin{aligned} \mathbb{P}(\mathbf{r} \rightarrow T_i) &= 1/2^i \quad \text{for } i = 1, 2, \dots, \nu^h - 1, \quad \text{and} \quad \mathbb{P}(\mathbf{r} \rightarrow T_0) = 1, \\ \mathbb{P}(\mathbf{r} \rightarrow v_i) &= 1/2^i \quad \text{for } i = 1, 2, \dots, \nu^h - 1, \quad \text{and} \quad \mathbb{P}(\mathbf{r} \rightarrow v_{\nu^h}) = 1/2^{\nu^h-1}. \end{aligned} \quad (66)$$

From each base node, the mass is then forwarded deterministically along its single outgoing edge to its single parent node and eventually reaches \mathbf{r} . Now every excursion starting from a base node v_i must pass through \mathbf{r} , and a return to v_j can occur only after exiting \mathbf{r} . Thus, the event of hitting v_j before returning to v_i for the first time after leaving v_i is equivalent to the event that an excursion initiated at \mathbf{r} reaches v_j before v_i . In particular,

$$\begin{aligned} Q_{G_{sc}}(v_i, v_j) &= \mathbb{P}[\tau_{v_j} < \tau_{v_i} | X_0 = v_i] = \mathbb{P}(\mathbf{r} \rightarrow v_j) = 1/2^j \quad \text{for } j = 1, 2, \dots, \nu^h - 1, \\ Q_{G_{sc}}(v_i, v_{\nu^h}) &= \mathbb{P}[\tau_{v_{\nu^h}} < \tau_{v_i} | X_0 = v_i] = \mathbb{P}(\mathbf{r} \rightarrow v_{\nu^h}) = 1/2^{\nu^h-1}. \end{aligned} \quad (67)$$

Similarly, starting at T_i , the probability of hitting T_j before returning to T_i , for $j < i$, is given by

$$\begin{aligned} Q_{G_{sc}}(T_i, T_j) &= \mathbb{P}\left[\mathbf{r} \rightarrow T_j \middle| \bigcup_{l=i+1}^{\nu^h} (T_i \rightarrow v_l) \text{ and } (v_l \rightarrow \mathbf{r})\right] \mathbb{P}\left[\bigcup_{l=i+1}^{\nu^h} (T_i \rightarrow v_l) \text{ and } (v_l \rightarrow \mathbf{r})\right] \\ &= \mathbb{P}(\mathbf{r} \rightarrow T_j); \end{aligned} \quad (68)$$

note that the complement event $\{\bigcap_{l=i+1}^{\nu^h} (T_i \not\rightarrow v_l) \text{ or } (v_l \not\rightarrow \mathbf{r})\}$ cannot happen. All of the preceding discussion identifies two relevant candidates for the graph diameter of G_{sc} : the distance between v_{ν^h-1} and v_{ν^h} , and the distance between T_{ν^h-2} and T_{ν^h-1} . All remaining pairs either involve larger values of ϕ or admit strictly larger probabilities Q_{sc} , and therefore yield smaller distances. For the first candidate distance, it follows from (6), (62), (67) that

$$E_{G_{sc}}(v_{\nu^h-1}, v_{\nu^h}) = \phi(v_{\nu^h-1}) Q_{G_{sc}}(v_{\nu^h-1}, v_{\nu^h}) = \phi(\mathbf{r})/2^{2(\nu^h-1)}. \quad (69)$$

For the second candidate, using (6), (62), (66), (68), we obtain

$$E_{G_{sc}}(T_{\nu^h-1}, T_{\nu^h-2}) = \phi(T_{\nu^h-1}) Q_{G_{sc}}(T_{\nu^h-1}, T_{\nu^h-2}) = \phi(\mathbf{r})/2^{2\nu^h-3}. \quad (70)$$

To calculate $\phi(\mathbf{r})$, we apply (58), (61), (62), and the normalization (9) to get

$$\begin{aligned} 1 &= \sum_{v \in V_{sc}} \phi(v) = \phi(\mathbf{r}) \cdot \left(2 + \sum_{i=1}^{\nu^h-1} \frac{1}{2^i}\right) + \sum_{l=0}^{\nu^h-1} \sum_{v: v \text{ in layer } l} \phi(v) \\ &= \phi(\mathbf{r}) \cdot \left(3 - \frac{1}{2^{\nu^h-1}}\right) + \sum_{l=0}^{\nu^h-1} \sum_{v: v \text{ in layer } l+1} \phi(v) = \phi(\mathbf{r}) \cdot \left(3 - \frac{1}{2^{\nu^h-1}}\right) + \nu^h \phi(\mathbf{r}) \\ &= \phi(\mathbf{r}) \cdot \left(3 - \frac{1}{2^{\nu^h-1}} + \nu^h\right). \end{aligned}$$

Consequently, $\nu^h \lesssim \phi(\mathbf{r}) \leq 1/3$. Therefore, by definition (7) and (69), (70), we conclude

$$\begin{aligned} \text{diam}(G_{sc}) &= \max\{d_{G_{sc}}(v_{\nu^h-1}, v_{\nu^h}), d_{G_{sc}}(T_{\nu^h-1}, T_{\nu^h-2})\} \\ &= \max\{\log(E_{G_{sc}}(v_{\nu^h-1}, v_{\nu^h})^{-1}), \log(E_{G_{sc}}(T_{\nu^h-1}, T_{\nu^h-2})^{-1})\} \lesssim \nu^h + \log \nu^h \lesssim \nu^h, \end{aligned}$$

which is (56). \square

Remark B.1. When restricted to Γ , $\text{diam}(\Gamma)$ is realized among pairs of computation nodes at layer $l = 1$. For any two such nodes v, w ,

$$E_{G_{sc}}(v, w) = \phi(v) \mathbb{P}\left(\bigcup_{w': w' \text{ child of } w} (\mathbf{r} \rightarrow w')\right).$$

Let v be the parent of $v_{\nu^h-\nu+1}, \dots, v_{\nu^h}$ and w the parent of $v_{\nu^h-2\nu+1}, \dots, v_{\nu^h-\nu}$ in the base layer. Observing that, from (66)

$$\mathbb{P}\left(\bigcup_{w': w' \text{ child of } w} (\mathbf{r} \rightarrow w')\right) \leq \mathbb{P}(\mathbf{r} \rightarrow T_{\nu^h-2\nu}) = 1/2^{\nu^h-2\nu}$$

and that the second inequality in (64) is attainable at v , we derive $E_{G_{sc}}(v, w) \in \mathcal{O}(2^{-2\nu^h+3\nu})$. Therefore, $\text{diam}(\Gamma) \gtrsim \nu^h$. Thus, from this perspective, passing to the larger graph G_{sc} does not change the order of the diameter.

Proof of Proposition B.1(ii). By definition (6), (7), for any $v \neq w \in \Gamma$,

$$\min_{v \neq w \in \Gamma} d_{G_{sc}}(v, w) = \min_{v \neq w \in \Gamma} \log \left(\frac{1}{\phi(v) Q_{G_{sc}}(v, w)} \right). \quad (71)$$

Here, the value $Q_{G_{sc}}(v, w)$ can be as large as 1, which occurs when w is the sole parent of v in the computation tree. It then follows from (59), (65) and the noted boundedness of $\phi(\mathbf{r})$ that $\phi(v) Q_{G_{sc}}(v, w) \leq 1/3$. Combined with (71), this implies $\min_{v \neq w \in \Gamma} d_{G_{sc}}(v, w) \geq 1$. Consequently, by (18), for any $v \neq w \in \Gamma$,

$$\|Q_\eta(v) - Q_\eta(w)\|_A \leq K_h = \frac{K_h d_{G_{sc}}(v, w)}{d_{G_{sc}}(v, w)} \leq \frac{K_h d_{G_{sc}}(v, w)}{\min_{v \neq w \in \Gamma} d_{G_{sc}}(v, w)} \leq K_h d_{G_{sc}}(v, w).$$

Setting $C_{Q_\eta} = K_h$ gives part (ii). \square

Proof of Proposition B.1(iii). Recall from Definition 2.1, f_{GCN} is given in terms of a p-hop graph convolution, using the Laplacian Δ_Γ , a 1-Lipschitz activation function σ , and network parameters (W_1, \dots, W_L) with network sizes $(\beta_1, \dots, \beta_L)$. Recall further that the network inputs lie in $\{0, 1\}^{s_{\nu, h}}$ and the outputs take values in $\mathbb{R}^{(\mathfrak{m}-1) \times s_{\nu, h}}$. Then from (11),

$$\|f_{\text{GCN}}(\Gamma, \cdot)\|_{\text{op}} \leq \|\Delta_\Gamma\|_{\text{op}}^{\text{p}(L-1)} \cdot \prod_{l=1}^L \|W_l\|_{\text{op}} \leq \|\Delta_\Gamma\|_{\text{op}}^{\text{p}(L-1)} \cdot \prod_{l=1}^L \beta_l. \quad (72)$$

From (4) and definition (10), we deduce (see also Remark B.2 below)

$$\|\Delta_\Gamma\|_{\text{op}} \leq \|\Delta_{G_{sc}}\|_{\text{op}} \leq \|\Phi_{G_{sc}}\|_{\text{op}} \cdot \left(1 + \frac{\|P_{G_{sc}}\|_{\text{op}} + \|P_{G_{sc}}^\top\|_{\text{op}}}{2} \right). \quad (73)$$

By the row-stochasticity of $P_{G_{sc}}$ (8), we have $\|P_{G_{sc}}\|_{\text{op}} = 1$. However, $\|P_{G_{sc}}^\top\|_{\text{op}} > 1$; particularly,

$$\|P_{G_{sc}}^\top\|_{\text{op}} = \max_{v \in V_{sc}} \sum_{w:(w,v) \in E_{sc}} \frac{1}{D_{G_{sc}}(w, w)} = \nu, \quad (74)$$

where the maximum is achieved at any computation node. From definition and (9), we have that $\|\Phi_{G_{sc}}\|_{\text{op}} \leq 1$. Substituting these estimates, together with (73), (74), back into (72), yields

$$\|f_{\text{GCN}}(\Gamma, \cdot)\|_{\text{op}} \leq \left(\frac{3+\nu}{2} \right)^{\text{p}(L-1)} \cdot \prod_{l=1}^L \beta_l, \quad (75)$$

which implies, for any $\mathbf{x}_1, \mathbf{x}_2 \in \{0, 1\}^{s_{\nu, h}}$,

$$\|f_{\text{GCN}}(\Gamma, \mathbf{x}_1) - f_{\text{GCN}}(\Gamma, \mathbf{x}_2)\|_\infty \leq \left(\frac{3+\nu}{2} \right)^{\text{p}(L-1)} \cdot \prod_{l=1}^L \beta_l \|\mathbf{x}_1 - \mathbf{x}_2\|_\infty. \quad (76)$$

By Definition 2.1, $\pi_v \circ f_{\text{GCN}}(\Gamma, \mathbf{0}) = \pi_w \circ f_{\text{GCN}}(\Gamma, \mathbf{0}) = 0$. Thus, for $v \neq w \in \Gamma$,

$$\begin{aligned} \|\pi_v \circ f_{\text{GCN}}(\Gamma, \mathbf{x}) - \pi_w \circ f_{\text{GCN}}(\Gamma, \mathbf{x})\|_\infty \\ \leq \|\pi_v \circ f_{\text{GCN}}(\Gamma, \mathbf{x}) - \pi_v \circ f_{\text{GCN}}(\Gamma, \mathbf{0})\|_\infty + \|\pi_w \circ f_{\text{GCN}}(\Gamma, \mathbf{0}) - \pi_w \circ f_{\text{GCN}}(\Gamma, \mathbf{x})\|_\infty. \end{aligned}$$

Therefore, from (76) and the fact that $\min_{v \neq w \in \Gamma} d_{G_{sc}}(v, w) \geq 1$,

$$\begin{aligned} \|\pi_v \circ f_{\text{GCN}}(\Gamma, \mathbf{x}) - \pi_w \circ f_{\text{GCN}}(\Gamma, \mathbf{x})\|_\infty &\leq 2 \left(\frac{3+\nu}{2} \right)^{\text{p}(L-1)} \cdot \prod_{l=1}^L \beta_l \cdot \frac{d_{G_{sc}}(v, w)}{\min_{v \neq w \in \Gamma} d_{G_{sc}}(v, w)} \\ &\leq 2 \left(\frac{3+\nu}{2} \right)^{\text{p}(L-1)} \cdot \prod_{l=1}^L \beta_l \cdot d_{G_{sc}}(v, w). \end{aligned} \quad (77)$$

Recalling that $\text{ilr}^{-1} : (\mathbb{R}^{\mathfrak{m}-1}, \|\cdot\|_2) \rightarrow (\Delta_{\mathfrak{m}}^\circ, \|\cdot\|_A)$ is an isometry, (77) then gives, for $v \neq w \in \Gamma$ and $h \in \mathcal{H}$,

$$\begin{aligned} \|\pi_v \circ h(\mathbf{x}) - \pi_w \circ h(\mathbf{x})\|_A &\leq (\mathfrak{m}-1)^{1/2} \|\pi_v \circ f_{\text{GCN}}(\Gamma, \mathbf{x}) - \pi_w \circ f_{\text{GCN}}(\Gamma, \mathbf{x})\|_\infty \\ &\leq 2(\mathfrak{m}-1)^{1/2} \left(\frac{3+\nu}{2} \right)^{\text{p}(L-1)} \cdot \prod_{l=1}^L \beta_l \cdot d_{G_{sc}}(v, w). \end{aligned} \quad (78)$$

Thus, taking $C_{\mathcal{H}}$ to be the constant multiplying $d_{G_{sc}}(v, w)$ in (78) proves part (iii). \square

Remark B.2. We estimate $\|\Delta_\Gamma\|_{\text{op}}$ by an upper bound of $\|\Delta_{G_{\text{sc}}}\|_{\text{op}}$. However, this entails no substantive loss as $\|P_{G_{\text{sc}}}\|_{\text{op}}, \|\Phi_{G_{\text{sc}}}\|_{\text{op}} \leq 1$, and the maximal diagonal entry of $\Phi_{G_{\text{sc}}}$ can be verified to be $\phi(\mathbf{r})$. Moreover, by (74), the maximum determining the value of $\|P_{G_{\text{sc}}}^\top\|_{\text{op}}$ is attained at a computation node in Γ .

With parts (i), (ii), (iii) established, this completes the proof of Proposition B.1. \square

C Proofs of Proposition 4.1 and (28)

Proof of Proposition 4.1. By [19, Proposition 2], we have the upper bound

$$\mathbb{P}(\bar{\tau} \leq \bar{n}) \leq 1 - \max_{i \in [k]} (1 - w_i)^{\bar{n}}. \quad (79)$$

Since the map $u \mapsto u^{\bar{n}}$ is non-decreasing on $\mathbb{R}_{\geq 0}$, we obtain

$$\mathbb{P}(\bar{\tau} \leq \bar{n}) \leq 1 - \max_{i \in [k]} (1 - w_i)^{\bar{n}} = 1 - \left(\max_{i \in [k]} (1 - w_i) \right)^{\bar{n}} = 1 - \left(1 - \min_{i \in [k]} w_i \right)^{\bar{n}}$$

as wanted. For the lower bound, observe that for each $i \in [k]$

$$\mathbb{P}(x_i \text{ never drawn before time } \bar{n}) = (1 - w_i)^{\bar{n}} \leq \left(1 - \min_{i \in [k]} w_i \right)^{\bar{n}}.$$

By interpreting $\mathbb{P}(\text{not complete before time } \bar{n}) = \mathbb{P}(\text{miss at least one point before time } \bar{n})$, we have from the union bound

$$\mathbb{P}(\bar{\tau} \leq \bar{n}) \geq 1 - k \left(1 - \min_{i \in [k]} w_i \right)^{\bar{n}},$$

which is lower bound in (27). The right-hand side above is maximized when $w_i = 1/k$ for all $i \in [k]$. For the final conclusion, it suffices to impose $1 - (1 - \min_{i \in [k]} w_i)^{\bar{n}} \leq \bar{\delta}$ in (27). \square

Before moving on to the proof of (28), we briefly show that indeed

$$1 - (k-1)^{\bar{n}} \left(\min_{i \in [k]} w_i \right)^{\bar{n}} - (k-1)(1 - \min_{i \in [k]} w_i)^{\bar{n}} \geq 1 - k \left(1 - \min_{i \in [k]} w_i \right)^{\bar{n}}.$$

Rearranging terms, this is equivalent to

$$(k-1)^{\bar{n}} \left(\min_{i \in [k]} w_i \right)^{\bar{n}} \leq \left(1 - \min_{i \in [k]} w_i \right)^{\bar{n}}. \quad (80)$$

Since $\min_{i \in [k]} w_i \leq 1/k$ and both sides of (80) are monotone in this quantity on $[0, 1/k]$, it suffices to check (80) at the maximal admissible value $\min_{i \in [k]} w_i = 1/k$, where it holds as an equality.

Proof of (28). We begin with a more general version of (79), that is

$$1 - \sum_{i=1}^k (1 - w_i)^{\bar{n}} \leq \mathbb{P}(\bar{\tau} \leq \bar{n}) \leq 1 - \max_{i \in [k]} (1 - w_i)^{\bar{n}}. \quad (81)$$

Define $f(\mathbf{p}) \stackrel{\text{def}}{=} 1 - \sum_{i=1}^k (1 - p_i)^{\bar{n}}$ for $\mathbf{p} \in \Delta_k \stackrel{\text{def}}{=} \{\mathbf{p} \in \mathbb{R}^k : p_i \geq 0 \text{ and } \sum_{i=1}^k p_i = 1\}$. We seek to maximize f on Δ_k , which we view as a compact, convex subset of \mathbb{R}^k . When imposing a uniform lower bound $p_i \geq \omega$, it suffices to consider the maximal value of f on the restricted simplex $\Delta_k^\omega \stackrel{\text{def}}{=} \{\mathbf{p} \in \mathbb{R}^k : p_i \geq \omega \text{ and } \sum_{i=1}^k p_i = 1\}$, which is a compact, convex subset of Δ_k , with $\omega \in [0, 1/k]$. Note that $\Delta_k^\omega = \emptyset$ for $\omega > 1/k$. Since $\bar{n} \geq k \geq 2$, the function f is continuous and concave on Δ_k and hence on Δ_k^ω . By Bauer's maximum principle [11], f attains its maximum on Δ_k^ω , and at least one such maximum is an extremal point of Δ_k^ω . Such an extremal point \mathbf{p} has one index j such that $p_i = \omega$ for all $i \neq j$ and $p_j = 1 - (k-1)\omega \geq \omega$. Without loss of generality, we take $j = 1$, yielding $\mathbf{p}^* = (1 - (k-1)\omega, \omega, \dots, \omega)$. Consequently,

$$f(\mathbf{p}^*) = 1 - (k-1)^{\bar{n}} \omega^{\bar{n}} - (k-1)(1 - \omega)^{\bar{n}} \geq f(\mathbf{p}) \quad \text{for all } \mathbf{p} \in \Delta_k^\omega. \quad (82)$$

Setting $\omega = \min_{i \in [k]} w_i$, and combining (82) with (81), we obtain (28), as desired. \square

References

- [1] Josh Achiam, Steven Adler, Sandhini Agarwal, Lama Ahmad, Ilge Akkaya, Florencia Leoni Aleman, Diogo Almeida, Janko Altenschmidt, Sam Altman, Shyamal Anadkat, et al. Gpt-4 technical report. *arXiv preprint arXiv:2303.08774*, 2023.
- [2] John Aitchison. The statistical analysis of compositional data. *Journal of the Royal Statistical Society: Series B (Methodological)*, 44(2):139–160, 1982.
- [3] Guillaume Alain and Yoshua Bengio. Understanding intermediate layers using linear classifier probes. *arXiv preprint arXiv:1610.01644*, 2016.
- [4] Akari Asai, Zequi Wu, Yizhong Wang, Avirup Sil, and Hannaneh Hajishirzi. Self-RAG: Learning to retrieve, generate, and critique through self-reflection. In *The Twelfth International Conference on Learning Representations*, 2024.
- [5] Patrice Assouad. Plongements Lipschitziens dans \mathbb{R}^n . *Bulletin de la Société Mathématique de France*, 111:429–448, 1983.
- [6] Daniel Bartl and Shahar Mendelson. Do we really need the Rademacher complexities? *arXiv preprint arXiv:2502.15118*, 2025.
- [7] Daniel Bartl and Shahar Mendelson. Uniform mean estimation via generic chaining. *arXiv preprint arXiv:2502.15116*, 2025.
- [8] Peter L Bartlett, Olivier Bousquet, and Shahar Mendelson. Local rademacher complexities. *The Annals of Statistics*, 33(4):1497–1537, 2005.
- [9] Peter L Bartlett and Shahar Mendelson. Rademacher and gaussian complexities: Risk bounds and structural results. *Journal of machine learning research*, 3(Nov):463–482, 2002.
- [10] David Bau, Bolei Zhou, Aditya Khosla, Aude Oliva, and Antonio Torralba. Network dissection: Quantifying interpretability of deep visual representations. In *Proceedings of the IEEE Conference on Computer Vision and Pattern Recognition (CVPR)*, pages 3319–3327, 2017.
- [11] Heinz Bauer. Minimalstellen von funktionen und extremalpunkte. *Archiv der Mathematik*, 9(4):389–393, 1958.
- [12] Alexandre Belloni, Victor Chernozhukov, and Lie Wang. Square-root lasso: pivotal recovery of sparse signals via conic programming. *Biometrika*, 98(4):791–806, 2011.
- [13] Yoshua Bengio, Geoffrey Hinton, Andrew Yao, Dawn Song, Pieter Abbeel, Trevor Darrell, Yuval Noah Harari, Ya-Qin Zhang, Lan Xue, Shai Shalev-Shwartz, et al. Managing extreme AI risks amid rapid progress. *Science*, 384(6698):842–845, 2024.
- [14] Beatrice Bevilacqua, Kyriacos Nikiforou, Borja Ibarz, Ioana Bica, Michela Paganini, Charles Blundell, Jovana Mitrovic, and Petar Veličković. Neural algorithmic reasoning with causal regularisation. In *International Conference on Machine Learning*, pages 2272–2288. PMLR, 2023.
- [15] Anselm Blumer, Andrzej Ehrenfeucht, David Haussler, and Manfred K Warmuth. Learnability and the Vapnik-Chervonenkis dimension. *Journal of the ACM (JACM)*, 36(4):929–965, 1989.
- [16] Nick Bostrom. *Superintelligence: Paths, Dangers, Strategies*. Oxford University Press, 2014.
- [17] Olivier Bournez, Johanne Cohen, and Adrian Wurm. A universal uniform approximation theorem for neural networks. In *Proceedings of the International Symposium on Mathematical Foundations of Computer Science (MFCS)*, Palaiseau, France, 2025.
- [18] Zachary M Boyd, Nicolas Fraiman, Jeremy Marzuola, Peter J Mucha, Braxton Osting, and Jonathan Weare. A metric on directed graphs and markov chains based on hitting probabilities. *SIAM Journal on Mathematics of Data Science*, 3(2):467–493, 2021.
- [19] Mark Brown, Erol A. Peköz, and Sheldon M. Ross. Coupon collecting. *Probability in the Engineering and Informational Sciences*, 22(2):221–229, 2008.

[20] Tom Brown, Benjamin Mann, Nick Ryder, Melanie Subbiah, Jared Kaplan, Prafulla Dhariwal, Arvind Neelakantan, Pranav Shyam, Girish Sastry, Amanda Askell, et al. Language models are few-shot learners. In *Advances in Neural Information Processing Systems (NeurIPS)*, 2020.

[21] Justin Chih-Yao Chen, Archiki Prasad, Swarnadeep Saha, Elias Stengel-Eskin, and Mohit Bansal. Magicore: Multi-agent, iterative, coarse-to-fine refinement for reasoning. In *Proceedings of EMNLP*, 2025.

[22] David Chiang. Transformers in uniform TC^0 . *arxiv*, 2024.

[23] Fan Chung. Laplacians and the cheeger inequality for directed graphs. *Annals of Combinatorics*, 9(1):1–19, 2005.

[24] Stephen Chung and Hava Siegelmann. Turing completeness of bounded-precision recurrent neural networks. *Advances in neural information processing systems*, 34:28431–28441, 2021.

[25] Alexis Conneau, Germán Kruszewski, Guillaume Lample, Loïc Barrault, and Marco Baroni. What you can cram into a single vector: Probing sentence embeddings for linguistic properties. *CoRR*, abs/1805.01070, 2018.

[26] Victor Contreras, Niccolò Marini, Lora Fanda, Gaetano Manzo, Yazan Mualla, Jean-Paul Calbimonte, Michael Schumacher, and Davide Calvaresi. A dixeire for extracting propositional rules from neural networks via binarization. *Electronics*, 11(24), 2022.

[27] Mark Craven and Jude Shavlik. Extracting tree-structured representations of trained networks. In D. Touretzky, M.C. Mozer, and M. Hasselmo, editors, *Advances in Neural Information Processing Systems*, volume 8. MIT Press, 1995.

[28] Damai Dai, Li Dong, Yaru Hao, Zhifang Sui, Baobao Chang, and Furu Wei. Knowledge neurons in pretrained transformers. In *Proceedings of the 60th Annual Meeting of the Association for Computational Linguistics (Volume 1: Long Papers)*, pages 8493–8502, Dublin, Ireland, 2022. Association for Computational Linguistics.

[29] Google DeepMind. Gemini: A family of highly capable multimodal models. *arXiv preprint arXiv:2312.11805*, 2023.

[30] Nils Detering, Luca Galimberti, Anastasis Kratsios, Giulia Livieri, and A Martina Neuman. Learning from one graph: transductive learning guarantees via the geometry of small random worlds. *arXiv preprint arXiv:2509.06894*, 2025.

[31] Jonas Erb and Nihat Ay. The information-geometric perspective of compositional data analysis. In *Advances in Compositional Data Analysis: Festschrift in Honour of Vera Pawlowsky-Glahn*, pages 21–43. Springer, 2021.

[32] Philippe Flajolet, Daniele Gardy, and Loÿs Thimonier. Birthday paradox, coupon collectors, caching algorithms and self-organizing search. *Discrete Applied Mathematics*, 39(3):207–229, 1992.

[33] Dobrik Georgiev Georgiev, Danilo Numeroso, Davide Bacciu, and Pietro Liò. Neural algorithmic reasoning for combinatorial optimisation. In *Learning on Graphs Conference*, pages 28–1. PMLR, 2024.

[34] Michael Greenacre. Compositional data analysis. *Annual Review of Statistics and its Application*, 8(1):271–299, 2021.

[35] Sariel Har-Peled and Manor Mendel. Fast construction of nets in low-dimensional metrics and their applications. *SIAM Journal on Computing*, 35(5):1148–1184, 2006.

[36] Songyan Hou, Parnian Kassraie, Anastasis Kratsios, Andreas Krause, and Jonas Rothfuss. Instance-dependent generalization bounds via optimal transport. *Journal of Machine Learning Research*, 24(349):1–51, 2023.

[37] Marek Karpinski and Angus Macintyre. Polynomial bounds for vc dimension of sigmoidal and general pfaffian neural networks. *Journal of Computer and System Sciences*, 54(1):169–176, 1997.

[38] Takeshi Kojima, Shixiang Shane Gu, Machel Reid, Yutaka Matsuo, and Yusuke Iwasawa. Large language models are zero-shot reasoners. *arXiv preprint arXiv:2205.11916*, 2022.

[39] Anastasis Kratsios, A Martina Neuman, and Gudmund Pammer. Tighter generalization bounds on digital computers via discrete optimal transport. *arXiv preprint arXiv:2402.05576*, 2024.

[40] Patrick Lewis, Ethan Perez, Aleksandra Piktus, Fabio Petroni, Vladimir Karpukhin, Naman Goyal, Heinrich Kütller, Mike Lewis, Wen-tau Yih, Tim Rocktäschel, et al. Retrieval-augmented generation for knowledge-intensive nlp tasks. *Advances in neural information processing systems*, 33:9459–9474, 2020.

[41] Wenhao Li, Anastasis Kratsios, Hrad Ghoukasian, and Dennis Zvigelsky. Certifiable reasoning is universal: A differentiable reasoning AI. *arXiv preprint*, 2026. Preprint.

[42] Daniel Lowd and Pedro Domingos. Learning arithmetic circuits. In *Proceedings of the Twenty-Fourth Conference on Uncertainty in Artificial Intelligence*, pages 383–392, 2008.

[43] Yao Ma, Xiaorui Liu, Neil Shah, and Jiliang Tang. Is homophily a necessity for graph neural networks? In *International Conference on Learning Representations*, 2022.

[44] Yao Ma and Jiliang Tang. *Deep learning on graphs*. Cambridge University Press, 2021.

[45] Wolfgang Maass, Georg Schnitger, and Eduardo D. Sontag. On the computational power of sigmoid versus boolean threshold circuits. In *Proceedings of the 32nd Annual Symposium on Foundations of Computer Science (FOCS)*, pages 767–776, 1991.

[46] Aman Madaan, Niket Tandon, Prakhar Gupta, Skyler Hallinan, Luyu Gao, Sarah Wiegreffe, Uri Alon, Nouha Dziri, Shrimai Prabhumoye, Yiming Yang, et al. Self-refine: Iterative refinement with self-feedback. *Advances in Neural Information Processing Systems*, 36:46534–46594, 2023.

[47] Ankur Arjun Mali, Alexander G Ororbia II, and C Lee Giles. A neural state pushdown automata. *IEEE Transactions on Artificial Intelligence*, 1(3):193–205, 2021.

[48] Kanti V Mardia and Peter E Jupp. *Directional statistics*. John Wiley & Sons, 2009.

[49] Susan Margulies and Jason Morton. Polynomial-time solvable# csp problems via algebraic models and pfaffian circuits. *Journal of Symbolic Computation*, 74:152–180, 2016.

[50] William Merrill and Ashish Sabharwal. The parallelism tradeoff: Limitations of log-precision transformers. *Transactions of the Association for Computational Linguistics*, 2023.

[51] William Merrill, Ashish Sabharwal, and Noah A. Smith. Saturated transformers are constant-depth threshold circuits. *Transactions of the Association for Computational Linguistics*, 2022.

[52] Assaf Naor and Ofer Neiman. Assouad’s theorem with dimension independent of the snowflaking. *Revista Matematica Iberoamericana*, 28(4):1123–1142, 2012.

[53] Ofer Neiman. Low dimensional embeddings of doubling metrics. *Theory Comput. Syst.*, 58(1):133–152, 2016.

[54] Chris Olah, Nick Cammarata, Ludwig Schubert, Gabriel Goh, Michael Petrov, and Shan Carter. Zoom in: An introduction to circuits. *Distill*, 5(3):e00024.001, 2020.

[55] Chris Olah, Arvind Satyanarayanan, Ian Johnson, Shan Carter, Ludwig Schubert, Katherine Ye, and Alexander Mordvintsev. The building blocks of interpretability. *Distill*, 3(3):e10, 2018.

[56] Soumik Pal and Ting-Kam Leonard Wong. Multiplicative schrödinger problem and the dirichlet transport. *Probability Theory and Related Fields*, 178(1):613–654, 2020.

[57] Vera Pawlowsky-Glahn and Juan José Egozcue. Compositional data and their analysis: an introduction. *Geological Society, London, Special Publications*, 264(1):1–10, 2006.

[58] Jorge Pérez, Javier Marinković, and Pablo Barceló. On the turing completeness of modern neural network architectures. In *International Conference on Learning Representations*, 2019.

[59] Alfréd Rényi. On a classical problem of probability theory. *Magyar Tudományos Akadémia Matematikai Kutató Intézetének Közleményei*, 6:215–220, 1958.

[60] Nikunj Saunshi, Nishanth Dikkala, Zhiyuan Li, Sanjiv Kumar, and Sashank J. Reddi. Reasoning with latent thoughts: On the power of looped transformers. In *The Thirteenth International Conference on Learning Representations*, 2025.

[61] Noah Shinn, Beck Labash, Ashwin Gopinath, and Karthik R. Narasimhan. Reflexion: Language agents with verbal reinforcement learning. In *Advances in Neural Information Processing Systems (NeurIPS)*, 2023.

[62] Hava T Siegelmann. *Neural networks and analog computation: beyond the Turing limit*. Springer Science & Business Media, 2012.

[63] Kai-Yeung Siu, Jehoshua Bruck, Thomas Kailath, and Thomas Hofmeister. Depth efficient neural networks for division and related problems. *IEEE Transactions on Information Theory*, 39(3):946–956, 1993.

[64] Max Sommerfeld and Axel Munk. Inference for empirical wasserstein distances on finite spaces. *Journal of the Royal Statistical Society Series B: Statistical Methodology*, 80(1):219–238, 2018.

[65] Zhao Song, Song Yue, and Jiahao Zhang. Thinking isn’t an illusion: Overcoming the limitations of reasoning models via tool augmentations. *arXiv preprint arXiv:2507.17699*, 2025.

[66] Benjamin Stucky and Sara Van De Geer. Sharp oracle inequalities for square root regularization. *Journal of Machine Learning Research*, 18(67):1–29, 2017.

[67] Cédric Villani et al. *Optimal transport: old and new*, volume 338. Springer, 2009.

[68] Guanzhi Wang, Yu Wang, Xinyi Liu, Shibin Liu, Yizhou Chen, Yiming Zhang, Jian Zhao, and Tong Zhang. Voyager: An open-ended embodied agent with large language models. In *International Conference on Learning Representations (ICLR)*, 2024.

[69] Xuezhi Wang, Jason Wei, Dale Schuurmans, Quoc V. Le, Ed H. Chi, Sharan Narang, Aakanksha Chowdhery, and Denny Zhou. Self-consistency improves chain of thought reasoning in language models. In *International Conference on Learning Representations (ICLR)*, 2023.

[70] Jason Wei, Xuezhi Wang, Dale Schuurmans, Maarten Bosma, Brian Ichter, Fei Xia, Ed Chi, Quoc V. Le, Denny Zhou, et al. Chain-of-thought prompting elicits reasoning in large language models. In *Advances in Neural Information Processing Systems (NeurIPS)*, 2022.

[71] Eric Zelikman, Yuhuai Wu, and Noah D Goodman. Star: Self-taught reasoner. In *Proceedings of the NIPS*, volume 22, 2022.